AMERICAN SOCIETY FOR MICROBIOLOGY | Clinical and Vaccine Immunology®

VACCINES

Impact of Poxvirus Vector Priming, Protein Coadministration, and Vaccine Intervals on HIV gp120 Vaccine-Elicited Antibody Magnitude and Function in Infant Macaques

Bonnie Phillips,[a] Genevieve G. Fouda,[b] Josh Eudailey,[b] Justin Pollara,[b] Alan D. Curtis II,[a] Erika Kunz,[b] Maria Dennis,[b] Xiaoying Shen,[b] Camden Bay,[c] Michael Hudgens,[c] David Pickup,[b] S. Munir Alam,[b] Amir Ardeshir,[d] Pamela A. Kozlowski,[e] Koen K. A. Van Rompay,[d] Guido Ferrari,[b] M. Anthony Moody,[b,f] Sallie Permar,[b,f] Kristina De Paris[a]

Department of Microbiology and Immunology and Center for AIDS Research, School of Medicine, University of North Carolina at Chapel Hill, Chapel Hill, North Carolina, USA[a]; Duke University Medical Center, Duke Human Vaccine Institute, Durham, North Carolina, USA[b]; Gillings School of Public Health and Center for AIDS Research, University of North Carolina at Chapel Hill, Chapel Hill, North Carolina, USA[c]; California National Primate Research Center, University of California at Davis, Davis, California, USA[d]; Department of Microbiology, Immunology and Parasitology, Louisiana State University Health Sciences Center, New Orleans, Louisiana, USA[e]; Department of Pediatrics, Duke University Medical Center, Durham, North Carolina, USA[f]

ABSTRACT Despite success in reducing vertical HIV transmission by maternal antiretroviral therapy, several obstacles limit its efficacy during breastfeeding, and breast-milk transmission is now the dominant mode of mother-to-child transmission (MTCT) of HIV in infants. Thus, a pediatric vaccine is needed to eradicate oral HIV infections in newborns and infants. Utilizing the infant rhesus macaque model, we compared 3 different vaccine regimens: (i) HIV envelope (Env) protein only, (ii) poxvirus vector (modified vaccinia virus Ankara [MVA])-HIV Env prime and HIV Env boost, and (iii) coadministration of HIV Env and MVA-HIV Env at all time points. The vaccines were administered with an accelerated, 3-week-interval regimen starting at birth for early induction of highly functional HIV Env-specific antibodies. We also tested whether an extended, 6-week immunization interval using the same vaccine regimen as in the coadministration group would enhance the quality of antibody responses. We found that pediatric HIV vaccines administered at birth are effective in inducing HIV Env-specific plasma IgG. The vaccine regimen consisting of only HIV Env protein induced the highest levels of variable region 1 and 2 (V1V2)-specific antibodies and tier 1 neutralizing antibodies, whereas the extended-interval regimen induced both persistent Env-specific systemic IgG and mucosal IgA responses. Antibody-dependent cell-mediated cytotoxicity (ADCC) antibodies in plasma were elicited by all vaccine regimens. These data suggest that infant immunizations beginning at birth are effective for the induction of functional HIV Env-specific antibodies that could potentially protect against breast milk transmission of HIV and set the stage for immunity prior to sexual debut.

KEYWORDS HIV vaccine, antibody responses, infant rhesus macaque model

In industrialized nations, mother-to-child transmission (MTCT) of human immunodeficiency virus (HIV) has been virtually eliminated by prenatal screening, the use of antiretroviral therapy (ART), and avoidance of breast feeding. Despite major progress, access to these MTCT prevention strategies remains highly variable in many resource-limited countries. Global ART coverage for prevention of MTCT (PMTCT) was estimated

Received 31 July 2017 **Accepted** 12 August 2017

Accepted manuscript posted online 16 August 2017

Citation Phillips B, Fouda GG, Eudailey J, Pollara J, Curtis AD, II, Kunz E, Dennis M, Shen X, Bay C, Hudgens M, Pickup D, Alam SM, Ardeshir A, Kozlowski PA, Van Rompay KKA, Ferrari G, Moody MA, Permar S, De Paris K. 2017. Impact of poxvirus vector priming, protein coadministration, and vaccine intervals on HIV gp120 vaccine-elicited antibody magnitude and function in infant macaques. Clin Vaccine Immunol 24:e00231-17. https://doi.org/10.1128/CVI.00231-17.

Editor Helene F. Rosenberg, IIS/LAD/NIAID/NIH

Address correspondence to Kristina De Paris, abelk@med.unc.edu.

at 80% in 2015. This coverage was ~90% in East and Southern Africa but remained below 50% in Asia and many other regions in Africa (1). In addition, HIV infection rates in women aged 15 to 24 only declined by 6% between 2005 and 2015 (2). Women experiencing acute HIV infection, especially late in pregnancy and/or during the breastfeeding period, are most likely to transmit infection to their babies (3). Even when mothers are diagnosed with HIV and started on ART during the breastfeeding period, the risk of MTCT remains high due to poor maternal adherence (4–6). Thus, in 2015, ~150,000 infants (~400 infants per day) became newly infected with HIV, half by breastfeeding (7, 8). Because breastfeeding is essential to provide nutrients and passive immunity against other pathogens that are prevalent in resource-poor countries, novel strategies are critically needed to eliminate breast milk transmission of HIV.

Ideally, a pediatric HIV vaccine would prevent breastfeeding infants born to HIV-infected women from becoming infected. Protection would have to be elicited rapidly in the face of continual exposures starting early after birth. Recent studies showed that HIV-infected infants could rapidly develop broadly neutralizing antibodies (9, 10), suggesting that despite their less mature immune system, infants can generate potent immune responses. However, the development of HIV immunogens that induce high titers of broadly neutralizing antibodies has proved challenging. In contrast, nonneutralizing antibodies with FcγR-mediated effector functions are easier to induce by vaccination. In addition, in the immune correlates analysis of the RV144 adult HIV vaccine trial, low levels of plasma antibodies that mediated antibody-dependent cell-mediated cytotoxicity (ADCC) were identified as a correlate of risk (11–16).

Simian immunodeficiency virus (SIV) infection of rhesus macaques (*Macaca mulatta*) is the most relevant animal model for the study of HIV pathogenesis and vaccine testing. All modes of MTCT of HIV (*in utero*, peripartum, and through breast milk) can be recapitulated in the SIV macaque model (17, 18), and immune development is similar in infant macaques and humans. Our goal was to identify a vaccine regimen that induces high-magnitude, persistent, ADCC-mediating, HIV Env-specific antibodies.

Based on prior observations, we selected 4 immunization regimens consisting of 2 immunogens, an HIV envelope (Env) protein and a poxvirus vector, which were administered on either an accelerated or extended time schedule. We utilized an Env protein immunogen because gp120 proteins delivered with adjuvant elicited long-lasting antibody responses in human infants (19). We selected HIV C.1086 Env derived from an HIV clade C transmitted founder virus because clade C is the most prevalent clade in sub-Saharan Africa, where the majority of pediatric HIV infections occur. In addition to the intramuscular (i.m.) route, C.1086 Env was also administered by the intranasal (i.n.) route to induce mucosal IgA, since breast milk acquisition of HIV occurs via mucosae. Indeed, prior pediatric SIV vaccine studies suggested that vaccine-induced mucosal IgA at the time of challenge correlated with control of viremia (20). The modified vaccinia virus Ankara (MVA) poxvirus vector expressing viral proteins was selected because of the modest protection with another poxvirus vector (canarypox) in the RV144 trial (21), the excellent safety record of poxviruses in human infants (22–25), and our previous demonstration that poxvirus-based vaccines elicited partial protection against oral SIV challenge in infant rhesus macaques (23). Finally, we compared an accelerated versus an extended-interval vaccination regimen because, while rapid elicitation of immune responses is needed, age-related changes in the developing infant immune system could improve the quantity and quality of vaccine-induced antibodies.

Four groups of infant macaques were used to test the immunogenicity of the different vaccine regimens. Three of these regimens (Env protein, prime/boost, and coadministration) were accelerated (3 immunizations at 3-week intervals), with the 4th group (extended interval) receiving the same regimen as the coadministration group but at 6-week intervals. The results are presented by comparing the 3 accelerated regimens, followed by a comparison of the accelerated and extended-interval coadministration groups. Our data show that the Env protein vaccination group elicited higher-avidity plasma IgG, the fastest kinetics of tier 1 neutralization, and the strongest

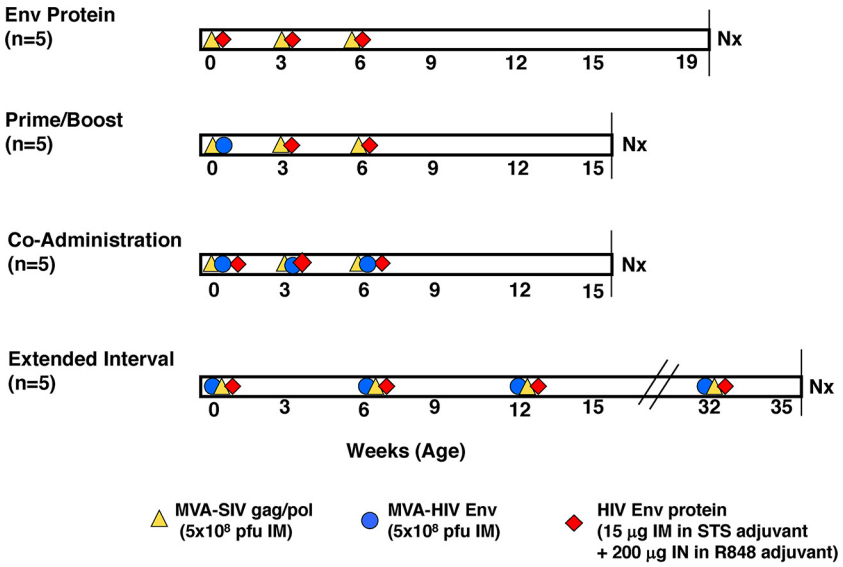

FIG 1 Vaccine regimens. Shown are the 4 vaccination groups and immunogens administered by the i.m. and i.n. routes. The timeline is expressed in weeks according to infant macaque age. Immunizations are indicated by symbols. Vaccine doses are listed at the bottom of the figure. Nx, necropsy.

variable region 1 and 2 (V1V2)-specific antibodies among the accelerated vaccine regimens. Yet, the extended-interval vaccine regimen was the only strategy that resulted in the development of both systemic IgG and mucosal IgA HIV Env-specific antibody responses, and it elicited tier 1 neutralizing and V1V2-specific antibodies similarly to the Env protein regimen.

RESULTS

HIV Env-specific plasma IgG responses. Figure 1 provides an overview of the study outline with the various vaccine regimens. The kinetics of gp120-specific plasma IgG development using the 3 accelerated vaccine regimens are illustrated in Fig. 2A. All groups, with the exception of the prime/boost group, began to produce IgG to consensus C gp120 after the first vaccination with C.1086 gp120 (Fig. 2A). The prime/boost group had detectable antibody responses after the second vaccination. Antibody responses to consensus C gp120 peaked 2 weeks after the third and final immunization in all accelerated vaccine cohorts and were of similar magnitudes at peak and thereafter. At euthanasia (week 15 for the prime/boost and coadministration groups and week 19 for the Env protein group), the gp120-specific IgG concentrations had decreased ~10-fold in all 3 groups (Fig. 2A).

We further tested whether this subtype C vaccine elicited Env-specific IgG that recognized different clades. All regimens induced plasma IgG that bound to clade A gp140, clade B gp140, and clade E gp120 (Fig. 2B). The responses to clade B gp140 were more variable than the other responses within most groups. Additionally, in relation to the levels of binding to clade C gp120, the median response to clade E gp120 was reduced by approximately a half log in the prime/boost group (Fig. 2B).

Epitope breadth of vaccine-induced plasma IgG. Antibodies elicited in the human RV144 HIV vaccine trial mediated ADCC, and responses specifically targeted V1V2 (15, 26), the third variable loop (V3) (27), and the first constant domain (C1) (14). Antibodies specific for the V2 epitope correlated with a decreased risk of HIV infection in these vaccinated adults (15). However, protection of human infants against vertical HIV transmission has been associated with maternal antibodies directed against the V3 loop (28). Using a binding antibody multiplex assay (BAMA), we found that peak plasma IgG responses to the C1, V2, and V3 epitopes of the C.1086 gp120 immunogen did not differ between groups (Fig. 2C). However, infants in the Env protein group had higher

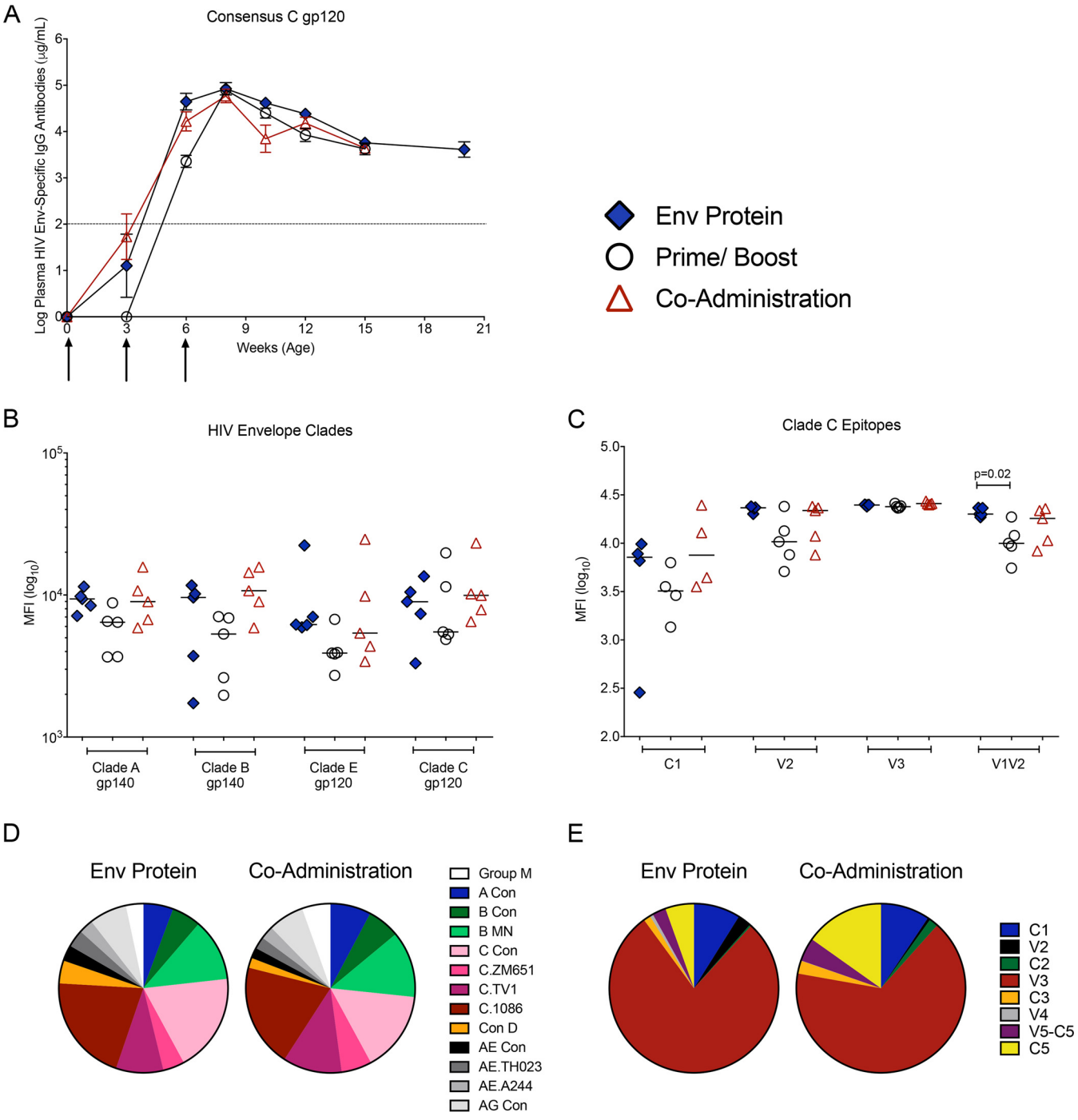

FIG 2 HIV Env-specific plasma IgG. (A) HIV gp120 consensus C-specific plasma IgG concentrations over time, measured by ELISA, are shown as mean values ± standard errors of the means (SEM). Arrows indicate the times of immunization. The dashed line represents the cutoff for HIV Env-specific IgG concentrations considered positive above the background. (B) Log_{10} MFI values for plasma IgG specific for clade A or clade B gp140 and clade E and clade C gp120 at peak (week 8, equal to 2 weeks after the 3rd immunization) that were measured by BAMA. (C) Specificities of clade C Env-specific plasma IgG determined at week 8 using BAMA. (D) Pie chart illustrating median signal intensities of IgG that recognize Env proteins from different clades by linear epitope mapping. (E) Pie chart summarizing results of linear epitope mapping of plasma IgG at week 8. Note that we did not perform linear epitope mapping for the prime/boost group because they showed slightly delayed induction of gp120-specific plasma IgG and generally had lower responses in the BAMA assay.

levels of plasma IgG against the V1V2 epitope than did the prime/boost group (P = 0.02) (Fig. 2C and Table S1 in the supplemental material).

Consistent with these BAMA data, the results from linear peptide array mapping showed that all groups recognized epitopes of other virus clades (Fig. 2D), and the

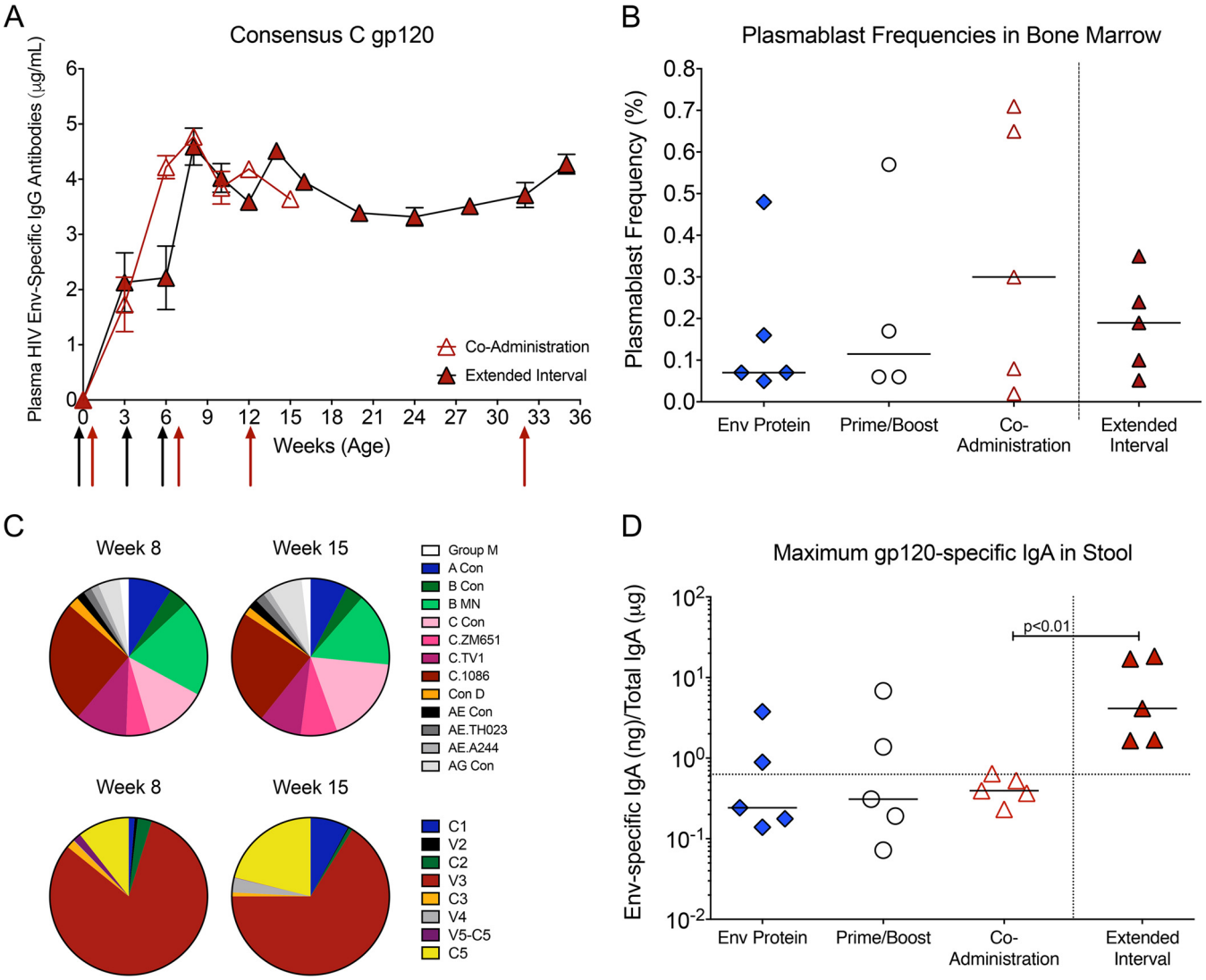

FIG 3 Env-specific antibody responses induced by the extended-interval regimen. (A) Comparison of mean consensus C gp120-specific plasma IgG concentrations in the 3-week accelerated coadministration group and 6-week extended-interval group. Black and red arrows indicate the times when immunizations were performed in the coadministration and extended-interval groups, respectively. (B) Median frequencies of plasmablasts in bone marrow of vaccinated animals at the time of euthanasia. Plasmablast frequencies are reported as percentages of Ki-67$^+$ IClgG$^+$ cells within the CD20$^{-/int}$ population. (C) Pie charts illustrating the median relative signal intensities of Env proteins of other clades or clade C Env epitopes recognized at weeks 8 and 15 by plasma IgG in animals of the extended-interval group as determined by linear epitope mapping. (D) Specific activities of C.1086 gp120-specific IgA, expressed as nanograms of anti-gp120 IgA per μg of total IgA, in fecal extracts prepared from stool samples. The dotted line indicates the cutoff for samples considered to be positive for C.1086 gp120-specific IgA.

majority of antibodies at the peak of the vaccine phase (2 weeks after the last immunization) targeted clade C V3 epitopes. However, we also detected antibodies against epitopes in the C1, V2, C2, V3, C3, V4, V5-C5, and C5 regions of Env (Fig. 2E and Table S2).

Effect of extending the time interval between immunizations on HIV Env-specific plasma IgG responses. Rationalizing that an increased interval between immunizations might allow for greater immune maturation and improved antibody responses, we compared the Env-specific antibody responses in the accelerated 3-week-interval coadministration group to the responses in the 6-week extended-interval coadministration group. Animals in both groups produced consensus C gp120-specific plasma IgG 2 weeks after the first immunization (Fig. 3A). Peak Env-specific IgG in the extended-interval group were observed 2 weeks after the last immunization (week 14), similar to what was seen in the coadministration group at week 8 (Fig. 3A). No evidence was

found of peak Env-specific IgG concentrations differing between groups ($P = 0.31$). The gp120-specific plasma IgG concentrations in the extended-interval group declined slightly after week 14, but these levels stabilized by week 20 and were maintained until week 32, suggesting that long-lived Env-specific plasma cells were generated. An additional boost at week 32 increased gp120-specific IgG to the levels observed at the time of peak response (Fig. 3A), indicating that gp120-specific memory B cells were also generated by the 6-week vaccination regimen. To confirm the generation of long-lived plasmablasts, we measured the frequencies of Ki-67-positive (Ki-67$^+$) B cells with no or only intermediate expression of CD20 (CD20$^{-/int}$) that tested positive for intracellular IgG but did not express surface IgG in bone marrow (Fig. 3B). The median plasmablast frequency in the bone marrow of animals receiving the accelerated coadministration regimen (0.26%) was higher than that observed in the Env protein-only (0.06%) or prime/boost (0.10%) group, but there was great variability within each group; the median plasmablast frequencies were similar between animals in the accelerated and extended-interval (0.19%) coadministration groups (Fig. 3B).

To further compare the specificities, magnitudes, and breadths of linear epitope binding between the coadministration and extended-interval groups, we mapped plasma antibodies at weeks 8 and 15 using a linear peptide array. The V3 epitope dominated the binding responses at week 8 in the extended-interval group (Fig. 3C) similarly to what was observed in the coadministration group (Fig. 2E). Although V3 responses still represented the dominant response by week 15, responses to C1 and C5 had increased (Fig. 3C). Cross-clade responses were detected to similar extents at both time points in the extended-interval group, with slight increases in anti-clade C consensus and clade AG IgG between weeks 8 and 15 (Fig. 3C). At week 15, cross-clade responses in the extended-interval group were comparable to those observed at week 8 in the coadministration group (Fig. 2D and E).

Induction of HIV Env-specific mucosal antibodies and B cell responses. The orogastrointestinal tract is an entry site for virus in breast milk. In previous studies, we found that vaccine-induced Env-specific IgA in saliva and intestinal secretions was associated with control of viremia in orally infected infant macaques (20, 29). Thus, an effective pediatric HIV vaccine may depend on the induction of local, mucosal IgA responses at the entry sites. Although we administered gp120 protein by both the i.m. and i.n. routes, the levels of C.1086 gp120-specific IgG and IgA were low or undetectable in saliva and did not differ between groups at the peak of the vaccine phase (data not shown). Similarly, the median values of gp120-specific IgA in stool samples from the Env protein, prime/boost, and coadministration vaccine groups were below the threshold for positivity. In contrast, all animals in the extended-interval group had low but detectable levels of gp120-specific IgA in their stool samples, indicating that an intestinal IgA response had been generated (Fig. 3D).

Avidity of vaccine-elicited anti-gp120 IgG. In previous SIV or simian-human immunodeficiency virus (SHIV) vaccine studies with adult macaques, the avidity of anti-Env serum IgG, as measured by chaotropic sodium thiocyanate (NaSCN) displacement enzyme-linked immunosorbent assay (ELISA), has been correlated with protection (30, 31). In these assays, antibody avidity has been reported as the avidity index (AI), and antibodies with an AI of <30, 30 to 50, or >50 have been considered to be of low, intermediate or high avidity, respectively (32). In the current study, the median AI values of C.1086 gp120-specific plasma IgG at peak (2 weeks after the third immunization) were in the low range for animals in the prime/boost (AI = 24) and Env protein (AI = 27) groups, whereas animals in the coadministration group developed antibodies with intermediate avidity (AI = 37) (Fig. 4A). The extended-interval coadministration regimen induced antibodies with the highest avidity (AI = 47) (Fig. 4A).

We also measured antibody avidity using surface plasmon resonance (SPR), which may more accurately measure avidity to conformational epitopes. Using SPR, the median avidity score of C.1086 gp120-specific antibodies was found to be higher in the Env protein group than in the prime/boost and coadministration groups (Fig. 4B).

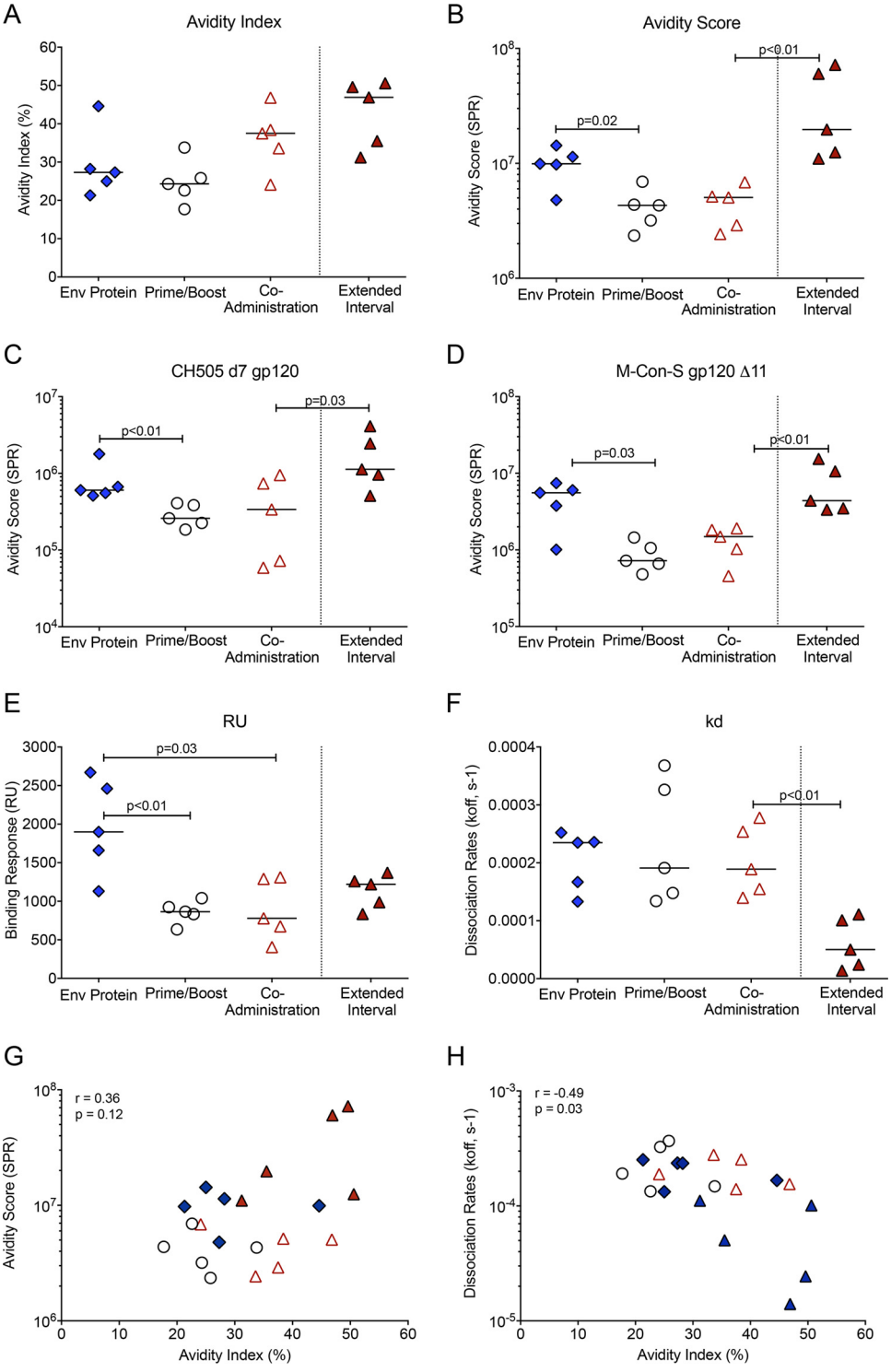

FIG 4 Plasma IgG avidity at the time of peak responses. (A) The avidity index for C.1086 gp120-specific IgG in plasma of animals within each vaccine regimen at peak was measured using the NaSCN displacement ELISA. (B) The avidity score, determined by SPR, is shown for each animal at peak. (C and D) The differences between the Env protein and prime/boost groups and between the accelerated and extended-interval coadministration groups for IgG avidity scores to clade C CH505 gp120 (C) and group M Con-S A11 gp120 (D) are illustrated. (E and F) The respective maximum binding responses and dissociation rates that determined the C.1086 gp120 avidity scores presented in panel B are shown. (G and H) The results of Spearman rank tests for the C.1086 gp120 avidity index and avidity score (G) and for the C.1086 gp120 avidity index and the dissociation rate measured by SPR (H) are shown. The symbols are as defined in the keys in Fig. 2A and 3A.

Animals in the Env protein group also had higher avidity scores to clade C CH505 gp120 and the group M Con-S gp120Δ11 protein (Fig. 4C and D). Between the coadministration regimens, the extended-interval regimen induced antibodies with higher avidity than the accelerated regimen to C.1086 gp120, CH505 gp120, and M Con-S gp120Δ11 ($P < 0.01$, $P = 0.03$, and $P < 0.01$, respectively) (Fig. 4B to D). The higher avidity of the C.1086 gp120-specific antibodies in the extended-interval group was attributed to a very low dissociation rate, as the maximum binding responses did not differ greatly from those in the coadministration group (Fig. 4E and F).

It is currently unknown which of these avidity assays best predicts protection, because the results of SPR have not yet been reported for vaccine/challenge studies with macaques. For this reason, we provide both measurements as a reference point for both prior and future studies. Although there was no correlation between avidity indices and avidity scores (Fig. 4G), the avidity indices were inversely correlated with dissociation rates in the SPR assay (Fig. 4H).

ADCC activity of vaccine-induced HIV Env-specific antibodies. In the RV144 trial, plasma ADCC activity was inversely correlated with the risk of HIV infection (15). We measured plasma IgG ADCC activities against the C.1086 gp120 immunogen and against clade C SHIV1157idp3N4 gp120 2 weeks after the 3rd immunization (week 14 for extended-interval group; week 8 for all others). All regimens induced similar titers of ADCC-mediating plasma antibodies to C.1086 gp120 (Fig. 5A). In response to heterologous SHIV1157idp3N4 gp120, the prime/boost group had the lowest ADCC activity and the extended-interval group the highest (Fig. 5B). We also noted a correlation between the C.1086 gp120 avidity indices and ADCC activity measured using SHIV1157ipd3N4 gp120 (Fig. 5C). Thus, the extended-interval regimen elicited the most consistent ADCC responses against both autologous and heterologous Env proteins.

Tier 1 virus neutralizing plasma antibodies. We tested the ability of vaccine-induced antibodies to mediate virus neutralization and found that all vaccination strategies induced neutralizing antibodies against the tier 1 clade C virus MW965 (Fig. 5D). Neutralizing antibodies were detectable after 2 immunizations (at week 6) in all infants in the Env protein group and in 4 of 5 infants in the coadministration group. However, 3 immunizations were required to induce measurable levels of neutralizing antibodies in all of the prime/boost animals (Fig. 5D). In most animals, peak neutralizing antibody responses were observed 2 weeks after the third immunization (week 8); however, in some animals, neutralization titers increased until week 12 (data not shown). When we compared the maximum titers for each animal, the median peak neutralizing antibody titer was higher for animals in the Env protein group than for animals in the prime/boost group (Fig. 5D). None of the three vaccine regimens induced substantial levels (3-fold above background) of tier 2 autologous neutralizing antibodies (data not shown).

Similar to our findings for the accelerated vaccine regimens (Fig. 5D), neutralizing antibodies against the clade C tier 1 virus MW965 peaked 2 weeks after the last immunization in the extended-interval group (Fig. 5E). Although neutralizing antibody responses declined, detectable neutralizing antibody persisted and was boosted after the 4th immunization at week 32 (Fig. 5E). There was a trend ($P = 0.0952$) toward higher maximum neutralizing antibody responses in the extended-interval group than in the accelerated coadministration group (Fig. 5E and Table S3).

HIV Env-specific B cells in tissues at time of euthanasia. Next, we investigated whether differences in gp120-specific IgG levels in plasma and gp120-specific IgA in stool were reflected by the frequencies of gp120-specific B cells in tissues. We analyzed spleen samples as a representative systemic lymphoid tissue. Lymph nodes (LNs) draining the oral cavity (retropharyngeal or submandibular) and intestinal tissues (colon) were studied, as these tissues represent potential sites of viral entry in infants orally exposed to virus in breast milk. At necropsy, the coadministration group had the highest frequencies of HIV Env-specific B cells in the spleen, both in total B cells and the

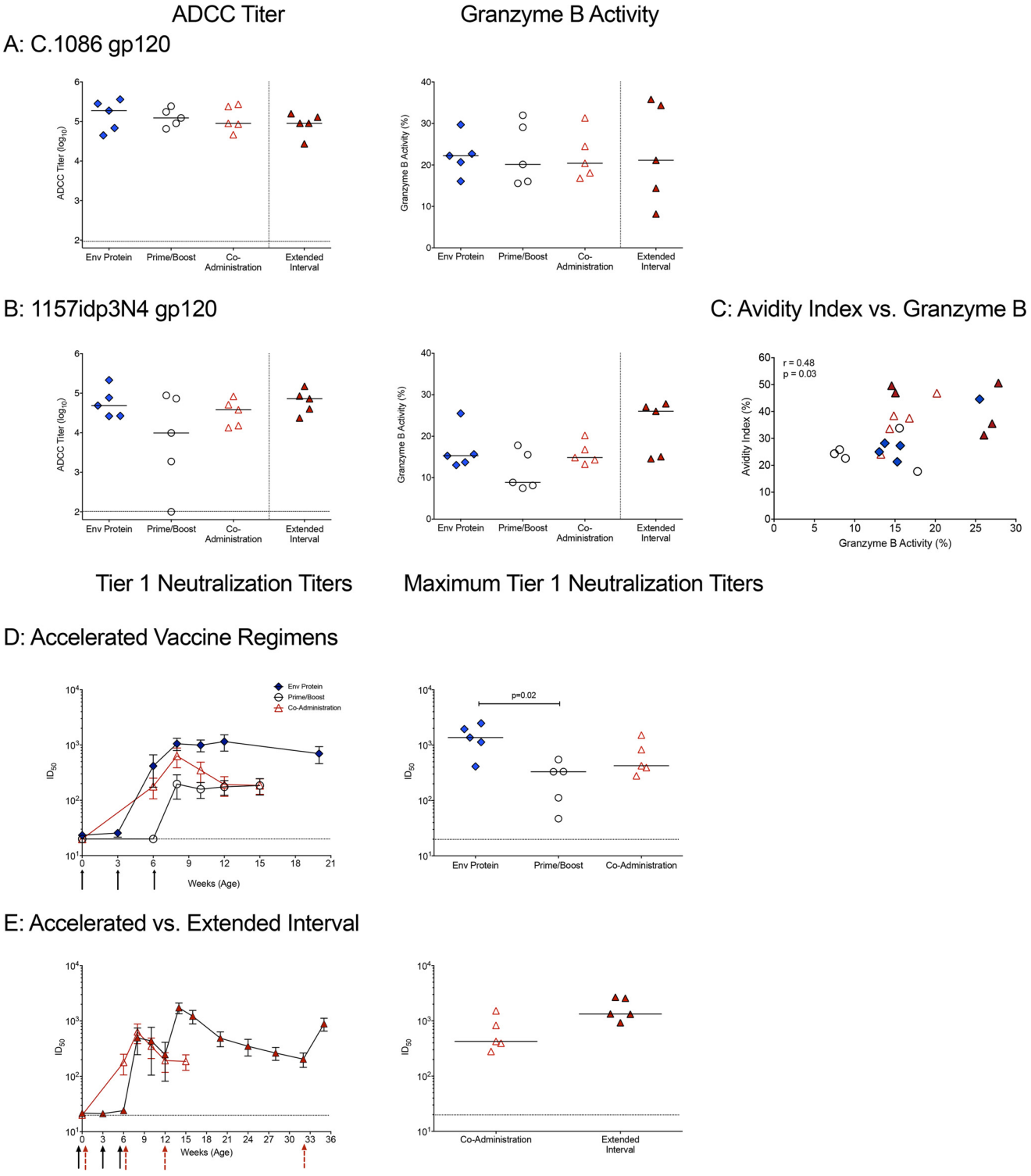

FIG 5 ADCC activity and tier 1 neutralizing antibodies in plasma. (A) Plasma was tested for the ability to mediate ADCC against cells coated with the C.1086 gp120 immunogen. Shown are the $\log_{10}$ reciprocal endpoint titers of plasma with detectable ADCC activity for each animal in the four vaccine groups. The horizontal dashed line represents the cutoff for positivity. Plasma samples from the extended-interval group at week 14 or from the accelerated vaccine regimen groups at week 8 were tested. The granzyme B activity against C.1086 gp120 cells is expressed as the proportion of target cells positive for proteolytically active granzyme B out of the total viable target cell population after subtracting the background activity observed in wells containing effector and target cells in the absence of plasma. (B) The ADCC activities against target cells expressing the heterologous clade C SHIV 1157ipd3N4 gp120 are shown. (C) Spearman's rank correlations between the C.1086 gp120 IgG avidity indices and granzyme B activities against SHIV1157ipd3N4 gp120. (D) Development of plasma IgG that neutralize clade C MW965 infection of TZM-bl cells by 50%. Shown are mean 50% inhibitory concentrations (IC_{50}s) ± SD for each of the vaccine groups (left) and peak IC_{50} titers of neutralizing plasma antibodies (right) in animals of the accelerated vaccine groups. (E) Comparison of the kinetics and peak IC_{50} titers of neutralizing plasma antibodies between the accelerated and extended-interval coadministration vaccine regimens. The symbols are as defined in the keys in Fig. 2A and 3A.

memory B cell populations (Fig. 6A). In contrast, the frequency of Env-specific B cells in oral lymph nodes was highest in the Env protein group (median frequency, 0.91%) and lowest in the prime/boost group (0.02%) (Fig. 6B). An intermediate frequency was observed in the coadministration group (0.63%), and this frequency was higher than that in the prime/boost group (Fig. 6B). These frequencies paralleled those of gp120-specific $CD27^+$ memory B cells (Env protein group, 4.35%; prime/boost group, 0.68%; and coadministration group, 3.9%) (Fig. 6B). In animals of the extended-interval group, we analyzed gp120-specific B cells in tissue biopsy specimens at week 15 and at the time of euthanasia. At week 15, we collected a peripheral LN, because LNs draining the oral cavity are too deep to be excised from small infant macaques. The median gp120-specific B cell frequency in the axillary LNs was slightly higher than that observed in oral LNs (Fig. 6C). At the time of euthanasia, the frequencies of gp120-specific total and memory B cells in oral LNs were lower in animals receiving the extended-interval than in those receiving the accelerated coadministration vaccine regimen, whereas the opposite was observed for the spleen samples (Fig. 6C).

In the colon, gp120-specific B cells were only generated by the extended-interval regimen (Fig. 6D and E), a finding consistent with the above-described observation that this regimen was best for the induction of gp120-specific IgA in stool samples. Env-specific B cells were also found in intestinal biopsy specimens of animals in the extended-interval group 3 weeks after the 3rd immunization (week 15) (Fig. 6D and E), the caveat being that antigen-specific intestinal B cells in the extended-interval group were measured 3 weeks after the third and fourth immunizations, times close to expected peak responses, whereas Env-specific B cells in all other vaccine groups were measured >8 weeks after the third immunization.

T_{FH} cell IL-4 secretion in lymph nodes and spleen. T follicular helper (T_{FH}) cells play an indispensable role in the activation of B cells and the production of high-affinity antibodies. Specifically, interleukin-4 (IL-4) production can drive B cell proliferation and class switching. Therefore, we determined the frequencies of T_{FH} cells, as well as their capacity to secrete IL-4, and tested for a correlation between T_{FH} cells and HIV Env-specific B cell responses.

In both the oral lymph nodes and spleens, T_{FH} frequencies at necropsy were similar in all animals independent of the vaccine regimen (Fig. 7A). However, the vaccine regimens differentially affected the *in vitro* function of T_{FH} cells. The Env protein group had higher frequencies of IL-4-producing (IL-4^+) T_{FH} cells in oral lymph nodes than animals in the coadministration and prime/boost groups (Fig. 7B). Similarly, animals receiving the Env protein vaccine regimen also had higher frequencies of IL-4-producing T_{FH} cells in the spleen than the prime/boost cohort (Fig. 7B). The extended-interval group had lower T_{FH} frequencies in the spleen than the accelerated coadministration group; however, both in spleens and in lymph nodes, the frequencies of IL-4-producing T_{FH} cells in animals receiving the coadministration vaccine were higher in the extended-interval than in the accelerated group (Fig. 7A and B).

To further examine the importance of IL-4-producing T_{FH} cells for HIV Env-specific antibody function, we tested for correlations between IL-4^+ T_{FH} cells and antibody avidity, neutralizing antibodies, and ADCC activity. In spleens and in oral LNs, there were positive correlations between the frequencies of IL-4-producing T_{FH} cells and the avidity indices of C.1086-specific plasma IgG (Fig. 7C); a similar correlation was not observed when we applied the avidity score ($P = 0.23$; data not shown). We also observed a positive correlation between IL-4-producing T_{FH} cells in tissues and maximum tier 1 neutralizing plasma antibodies (Fig. 7D). Consistent with the correlation between the C.1086 gp120 avidity indices and ADCC activities measured using SHIV1157ipd3N4 gp120 (Fig. 5C) and the correlation between avidity indices and IL-4-positive T_{FH} cells (Fig. 7C), there was also a positive correlation between IL-4-producing T_{FH} cells and ADCC activities measured using SHIV1157ipd3N4 gp120 (Fig. 7E).

SIV Gag and HIV Env-specific T cell responses in mesenteric lymph nodes. Should a vaccine not be able to protect against infection, virus-specific T cell responses

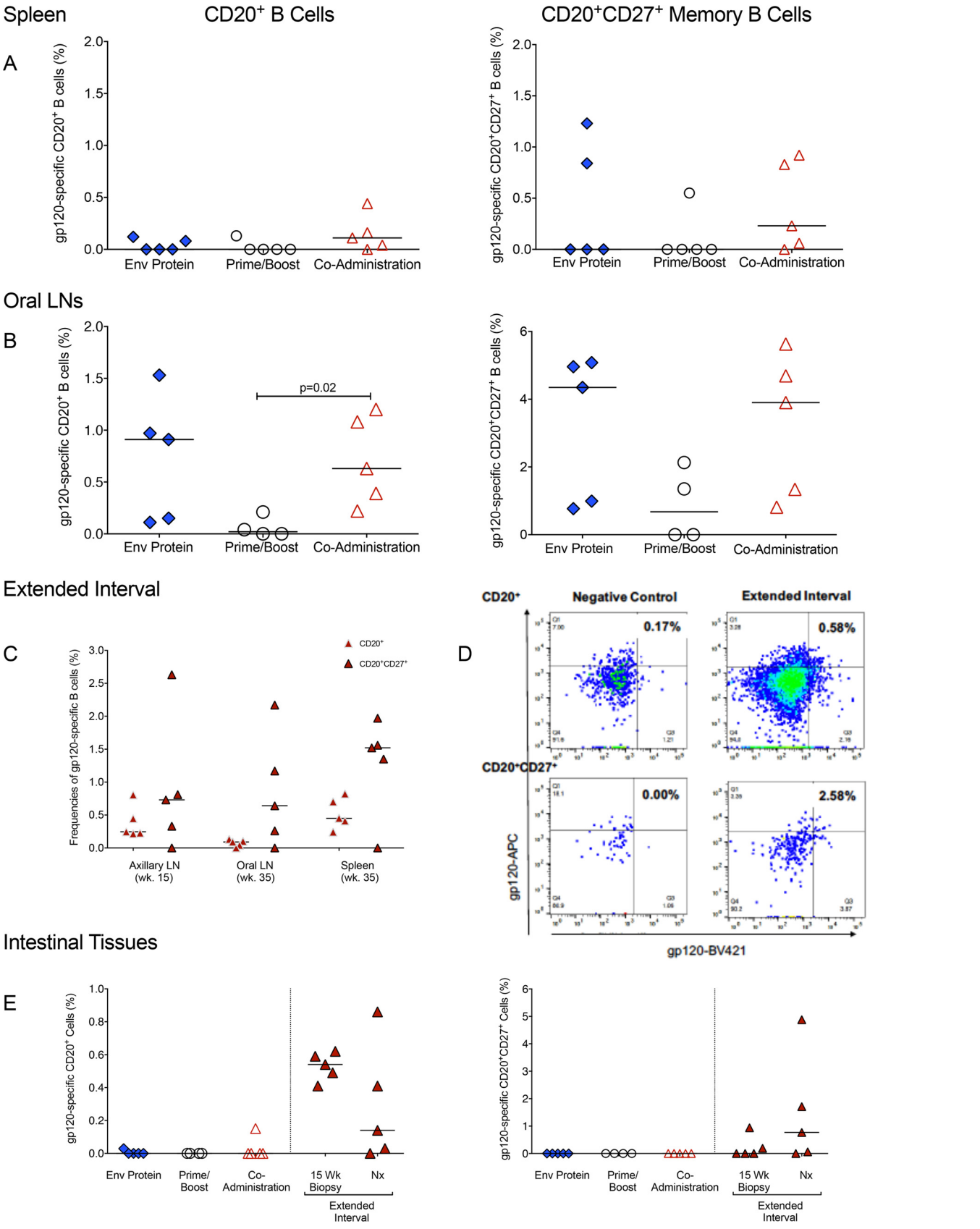

FIG 6 Tissue HIV Env-specific B cells. (A and B) HIV gp120-specific B cell frequencies in spleens (A) and oral lymph nodes (B) at necropsy were determined by flow cytometry, and the results are reported as percentages of total CD20$^+$ B cells or as percentages of memory CD20$^+$ CD27$^+$

(Continued on next page)

are essential to control early virus replication, thereby reducing virus dissemination and the size of the viral reservoir. All vaccine regimens were able to induce SIV Gag-specific $CD4^+$ and $CD8^+$ T cell responses in mesenteric LNs (Fig. 8A). The responses did not differ in magnitude or cytokine profile between the 3 groups receiving an accelerated vaccine regimen or between the groups receiving the accelerated and extended-interval coadministration regimens. Similar data were obtained when we measured HIV Env-specific $CD4^+$ and $CD8^+$ T cell responses in mesenteric LNs (Fig. 8B).

DISCUSSION

Based on the antibody responses associated with protection in the RV144 trial and the short window of time that infants have to induce immunity before exposure and potential HIV infection occur (8, 15), the goal of the current study was to identify a pediatric vaccine regimen that could induce durable high concentrations of HIV Env-specific antibodies with robust ADCC in plasma, in addition to eliciting Env-specific mucosal IgA responses in the gastrointestinal tract. We compared three accelerated regimens (3-week intervals), all beginning during the first week of life, to determine which would produce the greatest magnitude and/or functional capacity of HIV Env-specific plasma IgG. All vaccine regimens induced Env-specific plasma IgG in infant macaques. However, antibody function differed depending on the regimen, as summarized in Table 1.

High concentrations of consensus C gp120-specific plasma IgG with similar cross-clade reactivities were observed in all groups that received the accelerated vaccinations. These results are consistent with our previous pediatric SIV vaccine studies documenting the induction of plasma IgG by accelerated vaccine regimens in infant macaques (20, 29, 33, 34). In contrast, mucosal IgA responses were not or only poorly induced by these 3 accelerated vaccine strategies.

In vaccine studies with adult macaques, the avidities of anti-Env serum IgG measured by NaSCN displacement ELISA have been correlated with the levels of ADCC activity (35) and protection against rectal or vaginal SHIV or SIV challenge (30, 31, 36, 37). In the current study, the avidity indices of C.1086 gp120-specific IgG measured in the NaSCN ELISA did not show evidence of differences between groups. However, using SPR, the Env protein vaccine regimen was found to have induced antibodies with significantly higher avidity to both C.1086 and CH505 gp120 than the prime/boost regimen. The different results obtained in these avidity assays may reflect differential induction of conformational and linear antibodies in the vaccine groups. It has been reported that the results of NaSCN avidity assays primarily reflect antibodies to linear epitopes, because chaotropic agents disrupt some conformational epitopes (38). Interestingly, antibody avidities measured in the NaSCN assay correlated better overall with ADCC activities. However, this does not mean that all ADCC antibodies generated in these animals were directed against linear gp120 epitopes. Conformational antibodies to the V3 loop have been found to survive urea treatment (38). As anti-V3 antibodies dominated the response to gp120 in all vaccine groups, these antibodies may have contributed to the ADCC activity in plasma. In the correlates analyses of the RV144 trial, serum IgG1 and IgG3 binding antibodies directed to the V1V2 regions of gp120, as well as serum antibodies mediating ADCC, were associated with reduced HIV acquisition (13, 14, 39). In this study, independent of the vaccine regimen, animals in all groups developed plasma ADCC antibodies to the C.1086 gp120 immunogen. Although we did not define ADCC epitope specificity, responses to V1V2 and C1 epitopes associated with ADCC-mediated protection in the RV144 trial were elicited in all vaccine groups (13, 14).

FIG 6 Legend (Continued)
B cells. (C) HIV Env-specific B cell frequencies in tissues of animals in the extended-interval group. (D) Representative fluorescence-activated cell sorting (FACS) plot of gp120-specific B cells in the colon of an animal in the extended-interval group. Background staining in an unvaccinated control animal is shown for comparison. Reported values for total and memory B cells specific for HIV gp120 were corrected for nonspecific staining in control samples. (E) Frequencies of HIV Env gp120-specific total $CD20^+$ B cells and memory $CD20^+$ $CD27^+$ B cells in the colons of vaccinated infant macaques. The symbols are as defined in the keys in Fig. 2A and 3A.

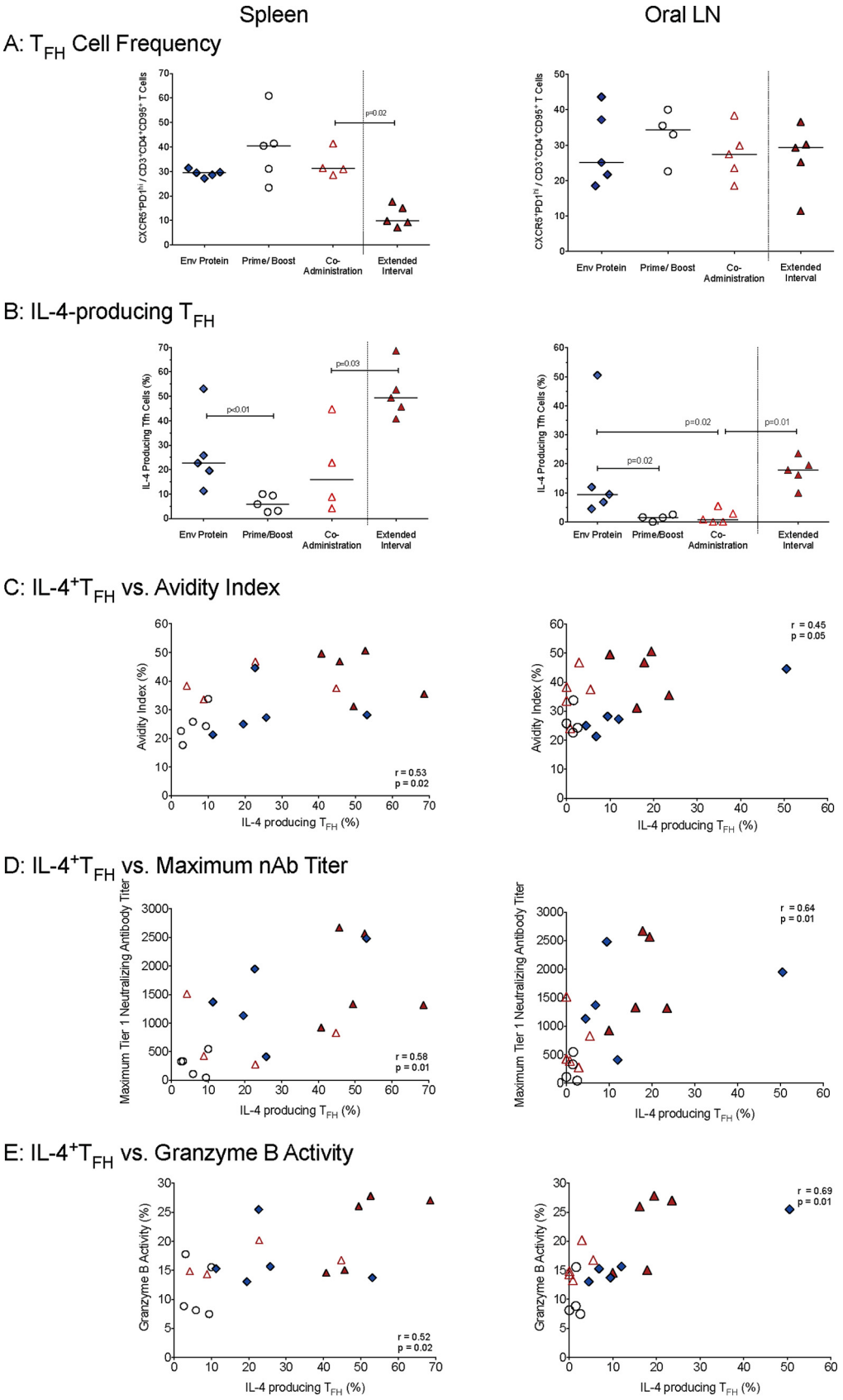

FIG 7 T follicular helper (T_{FH}) cell frequency and function. (A) The T_{FH} cell frequencies in animals of the various vaccine groups are reported as CXCR5$^+$ PD-1^{high} T cells within the population of CD95$^+$ CCR7^{low} CD4$^+$ T cells in oral lymph nodes

(Continued on next page)

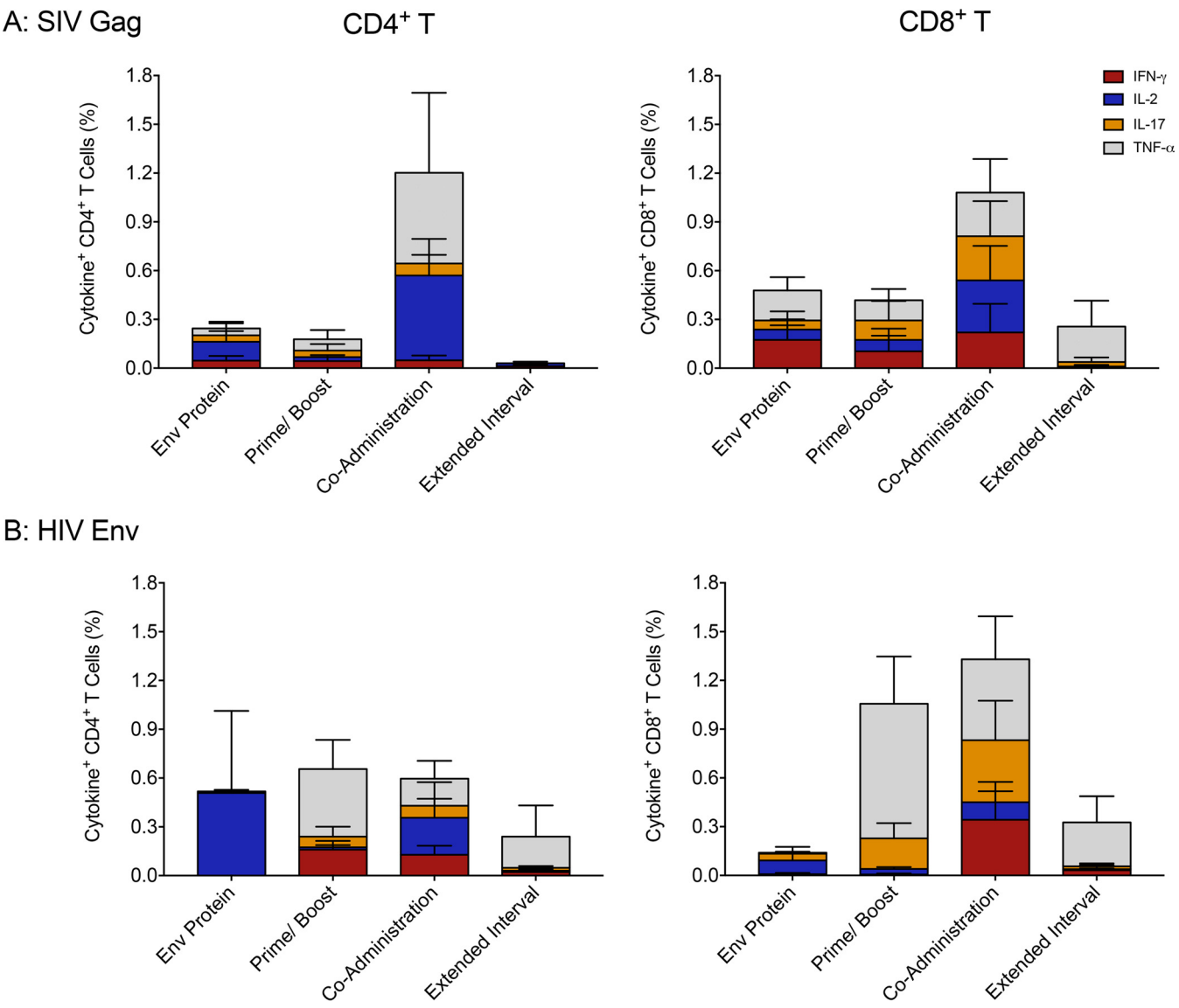

FIG 8 SIV Gag-specific and HIV Env-specific T cell responses. (A and B) Percentages of SIV Gag or HIV Env-specific $CD4^+$ (left) and $CD8^+$ T cells (right) in mesenteric LNs. Each bar represents the sum of the mean frequencies + SEM of IFN-γ, IL-2, IL-17, or TNF-α single-positive T cells in each group.

In addition, we found clear differences among groups when we measured tier 1 neutralizing antibodies to the clade C virus MW965. The prime/boost group showed delayed antibody kinetics and lower titers compared to those in the groups receiving the other accelerated regimens, whereas the Env protein regimen gave the highest and longest lasting responses.

Despite similar plasma levels of Env-specific IgG, the Env-specific B cell frequencies in spleens and oral LNs differed between the 3 accelerated vaccine regimens. Overall, Env-specific B cell frequencies were lower in spleens than in oral LNs. In the prime/boost group, only 1 of 5 infant macaques had detectable Env-specific B cells in oral LNs, whereas Env-specific B cells could be detected in all animals of the Env protein and

FIG 7 Legend (Continued)
or spleens. (B) The function of T_{FH} cells was assessed as percentages of T_{FH} cells producing IL-4 after *in vitro* stimulation. (C to E) Spearman's rank test correlations between frequencies of IL-4-producing T_{FH} cells in spleens or oral lymph nodes and plasma gp120-IgG avidities (C), maximum tier 1 plasma neutralizing antibodies (D), and levels of ADCC granzyme B activity directed against SHIV1157ipd3N4 (E) are shown. The symbols are as defined in the keys in Fig. 2A and 3A.

TABLE 1 Summary of vaccine-induced immune responses

Parameter	Response to indicated vaccine regimen			
	Accelerated interval			
	Env protein	Prime/boost	Coadministration	Extended interval coadmininistration
Plasma IgG				
Magnitude	++	++	++	++
Breadth	+++	+	++	++
Epitope recognition				
Magnitude	++	+	++	++
Breadth	++	+	++	++
Bone marrow plasmablasts	+	+	++	++
Mucosal IgA	+/−	+/−	+/−	+
Avidity	+++	+	++	++++
ADCC	++	+	++	++
Tier 1 neutralizing antibody	+++	+	++	++
gp120-specific B cells				
Spleen	++	+	++	++
LNs	++	+	++	++
Colon	+/−	+/−	+/−	+
T_{FH} cells				
Frequency	++	++	++	++
Function	++	+	++	++
SIV Gag-specific T cells				
Frequency	++	++	++	++
Function	++	++	++	++

coadministration groups. Although we did not determine antigen specificity, animals in the coadministration group also had a slightly higher median plasmablast frequency in the bone marrow. As described in "Statistical analysis" below, a studywise false discovery rate was utilized to account for multiple comparisons; for this false discovery rate (0.05), none of the null hypotheses tested in this paper would be rejected. Therefore, the reported unadjusted *P* values should be interpreted cautiously.

Among the accelerated vaccine regimens, vaccine-induced antibody breadth and function were lowest in the prime/boost group. The results for the Env protein strategy seemed to be slightly superior to the results for the coadministration group with regard to antibody avidity and tier 1 neutralization capacity. The finding that Env protein immunization can induce functional antibody responses in infant macaques is in agreement with data from studies by Fouda et al. (19), who showed in a retrospective analysis that the majority of human infants vaccinated with an MF59-adjuvanted gp120 protein vaccine maintained detectable plasma antibodies up to 1 year after their last immunization. Determining whether these antibodies can prevent oral virus transmission and which avidity assay best predicts protection need to be addressed in future vaccine/challenge studies with infant macaques. In human clinical HIV-1 vaccine trials in adults, strategies utilizing only Env protein did not elicit protection (40, 41).

Therefore, we decided to compare the accelerated coadministration regimen, which had also elicited some immune correlates of protection identified in the RV144 trial, to an extended-interval coadministration regimen. The peak plasma IgG did not differ between these two groups, but by testing an extended-interval group, we have shown antibody persistence up to 20 weeks after the last immunization, as well as the generation of Env-specific memory B cells that could be activated by a boost at this time. The plasma Env-specific IgG in the extended-interval group showed avidity

superior to that of such antibodies in the accelerated coadministration regimen. Furthermore, while animals in both groups developed plasma ADCC antibodies to the C.1086 gp120 immunogen, the median granzyme B activity against the heterologous SHIV1157idp3N4 Env was higher in infant macaques given the extended-interval regimen.

In addition, the extended-interval regimen, but not the accelerated coadministration regimen, also induced gp120-specific IgA responses in the gastrointestinal tract, suggesting that the development of intestinal IgA responses in infants may be optimal if vaccinations are performed at 6-week rather than 3-week intervals. We have previously shown that oral vaccine priming followed by systemic boosting in infants generates salivary or intestinal IgA responses that, albeit not protective against infection, correlate with control of viremia after oral SIV exposure (20, 29). Similarly, vaccine-mediated induction of Env-specific mucosal IgA responses at sites of SIV or SHIV challenge has been associated with protection, delayed rates of infection, or control of viremia in adult macaques (30, 36, 37, 42). Consistent with the induction of mucosal gp120-specific IgA, gp120-specific B cells in intestinal tissues were only detected in the extended-interval group. The detection of these cells was not simply due to a longer follow-up period after immunization, because Env-specific B cells in the colon were already detectable at week 15. Oral lymph nodes collected at the time of euthanasia in the extended-interval group had relatively low frequencies of Env-specific B cells (data not shown; median value, 0.1% of total B cells), but splenic Env-specific B cells were found at higher frequencies (median values, 0.45% of B cells and 1.5% of $CD27^+$ B cells).

The $CD4^+$ or $CD8^+$ T cell responses to HIV Env or SIV Gag did not differ between the groups. The observed SIV Gag-specific T cell responses were similar in magnitude and function to those observed in previously described accelerated prime/boost pediatric vaccine strategies (23, 29, 34). With the caveat that T cell responses were only analyzed at the time of euthanasia and only in mesenteric LNs, the extension of the immunization interval from 3 to 6 weeks did not appear to improve SIV Gag-specific or HIV Env-specific T cell responses.

In contrast, differences in vaccine-induced T_{FH} function resulting from the distinct vaccine regimens were associated with differences in vaccine-induced antibody responses, both in magnitude and in function. Thus, the frequency of IL-4-producing T_{FH} cells in tissues was predictive of gp120-specific plasma IgG avidity, maximum neutralizing tier plasma antibodies, and ADCC activity against heterologous SHIV1157ipd3N4, and animals with lower IL-4-producing T_{FH} cell frequencies also exhibited lower levels of plasma antibody function. Elucidating the enhancement of T_{FH} function via different vaccine regimens will be an important question to solve in order to develop an effective pediatric HIV vaccine.

Taken together, these data suggest that the dynamics of B cell and antibody circulation can be affected by the vaccine regimen and the vaccine interval. Acknowledging the caveat of relatively small group sizes, few studies have compared different vaccine regimens side-by-side in infants (43). Overall, the extended-interval regimen induced superior functional responses, such as broader ADCC activity and stronger intestinal IgA responses. The critical question remains as to whether these Env-specific antibody responses can prevent oral acquisition of immunodeficiency virus. An extended-interval regimen may be less efficient in protecting infants in the early postnatal phase. However, protection during this early risk period might be achieved through the administration of broadly neutralizing monoclonal antibodies (44) or long-acting antiretroviral drug formulations (45) shortly after birth. Thus, the vaccine regimen could potentially be tailored to fit the local availability of other early interventions and the expected duration of breastfeeding. In addition, the ability of a pediatric HIV vaccine to elicit persistent antiviral immune responses, as shown in the current study, would not only have the potential to protect against breast milk transmission of HIV but might provide protection into adulthood if a vaccine boost was given in early adolescence prior to sexual activity.

MATERIALS AND METHODS

Vaccine preparation. A recombinant modified vaccinia virus Ankara (MVA) (A711) expressing the HIV Env C.1086 gp120 protein (corresponding to residues 1 to 497 with a deletion of 6 amino acids [TVYYGV] and the mutation of K to N at position 160 [K160N]) was constructed as described previously for the construction of the gp140-expressing MVA virus A703 (46). Recombinant MVA expressing gp120 was cultured in BHK-21 cells and then partially purified by ultracentrifugation through 36% sucrose cushions as described previously (47). Monoclonal antibodies (VRC C 16H3) were used in Western blot analyses of proteins extracted from A711-infected BHK-21 cells to confirm the expression of the gp120 protein. The recombinant MVA expressing SIVmac239gag-pol was designed as described previously (46, 48). The recombinant C.1086_D7gp120K160N gp120 Env protein was produced in 293T cells as described previously (46).

Animals. Twenty SIV- and type D retrovirus-negative newborn Indian-origin rhesus macaques (*Macaca mulatta*) were hand reared in the nursery of the California National Primate Research Center (CNPRC, Davis, CA) in accordance with the American Association for Accreditation of Laboratory Animal Care standards. The *Guide for the Care and Use of Laboratory Animals* of the Institute for Laboratory Animal Research, National Research Council (49), and the *International Guiding Principles for Biomedical Research Involving Animals* (50) were strictly adhered to. All protocols were reviewed and approved by the University of California at Davis Institutional Animal Care and Use Committee prior to the initiation of the study. Animals were randomly assigned to the various groups between 3 and 7 days of age, when the first immunization was administered. For both vaccinations and sample collection, animals were anesthetized with 10 mg/kg of body weight of ketamine-HCl via the intramuscular (i.m.) route (Parke-Davis, Morris Plains, NJ).

Animal immunization regimens. As outlined in Fig. 1, infant macaques in the Env protein, prime/boost, and coadministration groups received immunizations at 0, 3, and 6 weeks of age. Infant macaques in all groups received MVA-SIVgag/pol i.m. (5×10^8 infectious units [IU] in 0.25 ml, split between quadriceps muscles) at every immunization time point to induce cellular immune responses, with the goal of limiting virus replication and dissemination. However, as our main goal was to induce functional ADCC-mediating HIV Env-specific antibody responses, the nomenclature of the group assignments was based on the various regimens used to elicit HIV Env-specific antibody responses. Infants in the Env protein group ($n = 5$) were vaccinated with C.1086 gp120 by both the i.m. (15 μg in 0.25 ml split between both gluteus muscles) and the i.n. (200 μg in 0.15 ml given dropwise with 30 s between drops and 3 drops per nostril) route. The i.m. protein immunizations contained 15 μg of Span85-Tween 80-squalene (STS) adjuvant as described previously (51), whereas Env protein by the i.n. route was given with 200 μg of the Toll-like receptor 7 and 8 (TLR7/8) agonist R848 (51). To enhance the induction of Env-specific antibody responses, infant macaques in the prime/boost group ($n = 5$) were primed i.m. with MVA-HIV Env at week 0 (5×10^8 IU in 0.25 ml split between the quadriceps) and then given C.1086 gp120 boosts at weeks 3 and 6. The coadministration group ($n = 5$) was vaccinated with both the MVA-HIV Env vector and the gp120 protein at weeks 0, 3, and 6. Animals were followed for 15 to 19 weeks, when they were euthanized to analyze vaccine-induced tissue responses. In addition, we included a group of infant macaques that received the same vaccine regimen as the coadministration group, but the immunization intervals were extended to 6 weeks (extended-interval group; $n = 5$). At week 32, infant macaques in the extended-interval group received a final boost, before being euthanized at week 35.

Collection and processing of blood and tissue specimens. Blood, saliva, and stool samples were collected before each immunization and then biweekly throughout the study. Saliva was collected with Merocel sponges (Beaver-Visitec, Waltham, MA), which were immediately snap-frozen. For stool collection, 2 to 3 g of fresh stool was added to 0.5% bovine serum albumin (BSA) in 5 ml sterile phosphate-buffered saline (PBS) supplemented with 1% protease inhibitor cocktail (product number P8340; Sigma). Saliva and stool samples were stored at −80°C.

Whole blood was collected, and plasma was obtained by centrifugation and stored at −80°C; peripheral blood mononuclear cells (PBMCs) were isolated as described previously (20, 29). At euthanasia, spleens, lymph nodes (LNs; axillary, mesenteric, submandibular, cervical, submental, and retropharyngeal), and intestinal tissues (colon and ileum) were collected and mononuclear cell (MNC) suspensions were prepared as described previously (20, 29).

At week 15, colon and axillary LN biopsy specimens were collected from animals of the extended-interval group. Prior to colonoscopy, animals were fasted for approximately 24 h. The morning of the procedure, the animals were sedated with ketamine and, if necessary, dexmedetomidine. Next, 30 ml/kg of a gastrointestinal lavage solution (GoLytely [Braintree Laboratories, Braintree, MA]; prepared by mixing with 1 liter of citrus-flavored water or Kool-Aid [Kraft Foods, Inc.]) was administered via naso- or orogastric tube. The remaining GoLytely solution was made available for the animal to drink. If the remaining solution was not consumed, the animal was sedated a second time (approximately 6 h later) to administer a second dose of GoLytely at 30 ml/kg to ensure that a total of 60 ml/kg was ingested. The use of GoLytely is important to get proper cleansing of the colon, without which there is more risk for perforation of the intestinal wall due to poor visibility (52). Animals were anesthetized with ketamine and dexmedetomidine during the colonoscopy procedure and monitored throughout the procedure by standard surgical monitoring (pulse, oximeter, and vitals check). The ultraslim pediatric endoscope (model number EG-1690K; Pentax Medical Company, Montvale, NJ) was lubricated, inserted into the rectum, and slowly advanced approximately 5 to 15 cm into the colon, depending on the animal's size. The left splenic flexure and right hepatic flexure were used to navigate to the proximal ascending colon. By performing proximal colonoscopy, we had access to a vast area (up to approximately 30 cm^2) of the

proximal and transverse colon to collect 5 to 8 pinch biopsy specimens. Animals were monitored until recovery from anesthesia and postoperatively for a minimum of 5 days. They also received ketoprofen at 2 mg/kg i.m. once daily for 3 days.

Purification of Rhesus IgG by affinity chromatography. A pool of IgG purified from plasma of two adult rhesus macaques previously vaccinated with HIV Env protein (RIVIG) (46) was used as the standard in the binding antibody multiplex assay (BAMA). IgG purification was performed as described previously (53). The total IgG concentration was determined by measuring absorbance at 280 nm with a NanoDrop 1000 spectrophotometer (Thermo Fisher Scientific).

BAMA for antibodies in plasma. BAMA was performed as described previously (54–59). Briefly, HIV antigens were conjugated to polystyrene beads (Bio-Rad) and the binding of plasma IgG to the bead-conjugated HIV antigens was measured. Positive controls included pooled purified IgG from HIV-positive persons (HIVIG; NIH AIDS Reagent Program), RIVIG, and a simian version of the HIV-specific human IgG neutralizing antibody b12 (B12R1). Beads and diluted plasma were incubated, and then bound IgG was detected using either a phycoerythrin (PE)-conjugated mouse anti-monkey IgG (Southern Biotech) at 4 μg/ml for macaque plasma, B12R1, and RIVIG or a PE-conjugated mouse anti-human IgG (Southern Biotech) at 2 μg/ml for HIVIG. The beads were washed and acquired on a Bio-Plex 200 instrument (Bio-Rad). IgG binding was expressed as mean fluorescence intensity (MFI). To control for nonspecific binding, the MFI of sample binding to unconjugated blank beads was subtracted from the MFI of each antigen. An HIV-specific antibody response was considered positive if it had MFI values above both (i) the mean MFI of preimmunized plasma samples at week 0 + 3 standard deviations (SD) and (ii) the lower detection limit of 100 MFI. The 50% effective concentrations (EC_{50}) and maximum MFI values of the standards (B12R1, HIVIG, and RIVIG) were tracked by Levy-Jennings charts to ensure consistency between assays.

Measurement of HIV Env-specific antibodies by ELISA. The plasma concentrations of HIV Env-specific antibodies were determined by ELISA (60). The 384-well plates were coated with 3 μg/ml of consensus C gp120 overnight at 4°C and then blocked with superblock (PBS plus 4% whey, 15% normal goat serum, and 0.5% Tween 20). After washing, serially diluted plasma was added to the plates. IgG were detected with peroxidase-labeled anti-monkey IgG (Southern Biotech), followed by tetramethylbenzidine (TMB; KPL) and stop solution. Immediately after the addition of the stop solution, absorbance was read at 450 nm. B12R1 was used as the standard (60). The concentration of HIV Env-specific IgG relative to the standard was calculated with a five-parameter fit curve using SoftMax Pro 6.3 software (Molecular Devices). To account for nonspecific binding, the positivity cutoff was selected as the concentration corresponding to 3 times the optical density (OD) of blank wells.

Plasma antibody linear epitope mapping. Plasma IgG linear epitope mapping by peptide microarray was performed as previously described (55, 61, 62) with minor modifications. Array slides were provided by JPT Peptide Technologies GmbH (Germany) by printing a library designed by B. Korber (Los Alamos National Laboratory) onto epoxy glass slides (PolyAn GmbH, Germany). The library contains overlapping peptides (15-mers overlapping by 12) covering 6 full-length gp160 consensus sequences (clades A, B, C, and D, group M, CRF1, and CRF2) and the gp120 sequences of 6 vaccine strains (MN, A244, Th023, TV-1, ZM651, and C.1086). Three identical subarrays, each containing the full peptide library, were printed on each slide. All array slides were blocked for 1 h, followed by 2 h of incubation with serum samples diluted 1:50 and a subsequent 45 min of incubation with goat anti-human IgG conjugated to Alexa Fluor 647 (AF647; Jackson ImmunoResearch, PA). The array slides were scanned at a wavelength of 635 nm with an InnoScan 710 scanner (Innopsys, Carbonne, France) using the extended dynamic range (XDR) mode. Images were analyzed using MagPix 7.4.1 software (Luminex Corporation) to obtain binding intensity values for all peptides. The binding values for preimmune serum from each animal were subtracted from the postimmunization binding values for each peptide. The binding magnitude to each epitope was defined as the highest binding to a single peptide within the epitope region.

BAMA for mucosal antibodies. Salivary and fecal antibodies to C.1086 gp120 were measured using BAMA. The gp120 protein (50 μg) was conjugated to 1×10^7 Bio-Plex magnetic beads (Bio-Rad) as described previously (63). Test samples were depleted of IgG using protein G-Sepharose. White microtiter plates previously blocked with PBS, containing 1% BSA, 0.05% Tween 20, and 0.05% azide (bead buffer), were loaded with 25 μl beads plus 25 μl diluted standard or mucosal fluid that had been clarified by centrifugation at 18,000 $\times$ *g* for 5 min. The standard was IgA or IgG that had been purified from serum of SHIV-infected macaques using peptide M agarose (Invivogen) or protein G-Sepharose (Genscript). The concentrations of the standards were adjusted so that they produced results analogous to those obtained in ELISA with plasma samples. The plate was mixed overnight at 4°C on an orbital shaker. The following day, the beads were washed with PBS containing 0.05% Tween 20, mixed for 30 min with bead buffer containing 2 μg/ml biotinylated goat anti-monkey IgA or IgG (Rockland Immunochemicals), washed, and mixed with 1/400 phycoerythrin-labeled Neutralite avidin for 30 min (Southern Biotech). After a final wash, the beads were resuspended in 100 μl of bead buffer and analyzed in a Bioplex 200 using Bioplex Manager software (Bio-Rad). To obtain specific activities, the concentrations of antibody were divided by the total IgA in the samples. Total IgA or IgG concentrations were measured by ELISA as described previously (64).

Avidity assays. The avidities of anti-C.1086 gp120 plasma IgG were measured using a sodium thiocyanate (NaSCN) displacement ELISA (20) and surface plasmon resonance (SPR). Briefly, for the NaSCN ELISA, plates coated with 100 ng per well of C.1086 gp120 were reacted overnight with the standard and plasma samples on two sides of the plate. The following day, wells on one side of the plate were treated with 1.5 M NaSCN for 10 min at 37°C. The plates were then developed using biotinylated affinity-purified goat anti-monkey IgG (Rockland Immunochemicals), neutralite avidin-peroxidase, and

TMB (SouthernBiotech). The avidity indices (AI) were calculated by dividing the concentrations of antibody in NaSCN-treated wells by the concentrations in untreated wells.

Surface plasmon resonance measurements of purified plasma IgG avidity were performed using a Biacore 4000 instrument (GE Healthcare). Using a multiplex array format (2 by 8), binding responses were measured by SPR in duplicate following immobilization by amine coupling of envelope protein (15) or capture of biotinylated antigens to immobilized streptavidin on series S CM5 sensor chips. Purified plasma IgG samples at 150 μg/ml (except for animal 45038, whose sample was used at 75 μg/ml due to insufficient IgG) were flowed (2.5 min) over duplicate spots of antigen, followed by a dissociation phase (postinjection/buffer wash) of 10 min. Nonspecific binding of a preimmune (time zero) sample was subtracted from the binding data for each postimmunization IgG sample. Data analyses were performed with BIAevaluation 4000 and BIAevaluation 4.1 software (BIAcore/GE Healthcare). Binding responses were measured by averaging postinjection response units (RU) over a 10-s window, and the dissociation rate constants (K_d [s^{-1}]) were measured during the postinjection phase (after stabilization of the signal). A positive response was defined when the RU was $\geq$10. The relative avidity binding score was calculated as follows: avidity score (RUs) = (binding RUs/K_d).

Neutralization assays. Neutralization of tier 1 and tier 2 clade C viruses by plasma was measured in TZM-bl cells by the reduction in luciferase reporter gene expression after a single round of infection, as described previously (65). Neutralization was assessed using MW965.LucR.T2A.ecto/293T (tier 1) and C.1086_B2.LucR.T2A.ecto/293T (tier 2) infectious molecular clones (IMCs). Broadly neutralizing antibody B12R1 or VRC01 was used as a positive control. The 50% inhibitory dose (ID_{50}) was calculated as the plasma dilution or antibody concentration that caused a 50% reduction in relative light units (RLUs) compared to the RLUs in the virus control wells after subtraction of cell control RLUs. The preimmunization time point (week 0) was used to measure background levels of neutralization.

Plasmablast analysis. Bone marrow cell suspensions were stained according to the protocol developed for rhesus macaques by Silveira et al. (66). Briefly, cells were stained for surface expression of CD3-PE-CF594, CD14-PE-CF594, CD16-PE-CF594, CD20-allophycocyanin (APC)-H7, CD11c-PE, CD123-PE, CD80-BUV395, and HLA-DR-BV711, with IgG-V450 (surface IgG [sIgG]), and for intracellular expression of Ki-67–fluorescein isothiocyanate (FITC) and IgG-AF700 (immune complex of IgG [ICIgG]). All antibodies were obtained from BD Biosciences. A live/dead discriminator dye was included in all panels. Samples (500,000 events) were acquired on a BD LSRFortessa instrument and analyzed using FlowJo software version 10 (TreeStar, Ashland, OR). Plasmablasts were defined as being negative for the lineage marker (CD3, CD14, and CD16), the dendritic cell markers CD11c and CD123, and sIgG but positive for HLA-DR ($HLA\text{-}DR^+$), Ki-67 ($Ki\text{-}67^+$), and ICIgG ($ICIgG^+$). Plasmablasts exhibited no or only intermediate expression of CD20 ($CD20^{-/int}$). In contrast to previous studies enumerating plasmablasts in PBMCs (66, 67), the bone marrow plasmablasts did not express CD80.

Detection of HIV Env-specific B cells. PBMCs and tissue MNC suspensions were treated with 5 μM Chk2 inhibitor II {2-[4-(4-chlorophenoxy)phenyl]-1H-benzimidazole-5-carboxamide; Sigma} and 1% BSA (Sigma) and blocked with 6.25 μg/ml anti-human CD4 antibody (BD) at 4°C for 15 min. We then costained cells with custom-conjugated BV421-gp120 (C.1086) and AF647-gp120 (C.1086) prepared as described previously (68). Paraformaldehyde-fixed samples were acquired on a BD LSRII Fortessa instrument and analyzed using FlowJo software version 10 (Tree Star, Ashland, OR). The following gating strategy was applied: lymphocytes were gated on singlets and live cells were selected to gate on $CD3^-$ cells (T cells), $CD14^-$ cells (monocytes/macrophages), or $CD20^+$ cells (B cells). B cells were further gated on $CD27^+$ memory B cells. Only B cells positive for both BV421-gp120 and AF647-gp120 were considered HIV Env specific, and these populations were normalized against data from nonimmunized control animals.

T follicular helper (T_{FH}) cell analysis. Tissue MNC suspensions containing 1.5×10^6 to 3.0×10^6 cells were resuspended in complete RPMI 1640 containing 0.5 μg/ml anti-CD28 antibody and 0.5 μg/ml anti-CD49d antibody (BD Biosciences). Cells were treated with 0.5× cell stimulation cocktail (eBioscience) or medium only and cultured for 6 h (37°C and 5% CO_2), with the addition of 1× brefeldin A (eBioscience) after the first hour. Cells were stained, and paraformaldehyde-fixed samples were acquired as described above. Gating was based on a lymphocyte gate, followed by gating on singlets and then live cells. $CD3^+$ $CD4^+$ T cells were further gated on $CD95^+$ $CCR7^{low}$ cells. T_{FH} cells were defined as $PD\text{-}1^{high}$ $CXCR5^+$ cells within the population of $CD95^+$ $CCR7^{low}$ $CD4^+$ T cells. Gates were based on fluorescence-minus-one (FMO) controls, and all cytokine analyses were performed after Boolean gating.

SIV Gag and HIV Env-specific T cell responses. Mesenteric LN cell suspensions were stimulated with 10 μg/2 $\times$ 10^6 cells of SIV Gag or HIV Env peptide pools (NIH Reference and Reagent Program) for 6 h, with brefeldin A being added for the last 5 h. Negative- and positive-control cultures included medium only or cell stimulation cocktail, respectively. Cells were stained as previously described (20, 34, 69), and 300,000 events were acquired on an LSRII Fortessa instrument and analyzed using FlowJo version 10 software. Gates were based on FMO controls, and cytokine analyses were performed after Boolean gating. The frequencies of gamma interferon (IFN-γ), IL-2, IL-17, and tumor necrosis factor alpha (TNF-α) single-positive $CD4^+$ or $CD8^+$ T cells are reported after subtracting background values obtained in medium-only cultures.

ADCC assay. The GranToxiLux (GTL) assay was used to detect plasma ADCC activity directed against $CCR5^+$ $CEM.NK^R$ T cells (AIDS Reagent Program; contributed by Alexandra Trkola) coated with the C.1086 gp120 or clade C SHIV1157ipd3N4 gp120 as described previously (70). ADCC activity was measured in 4-fold serial plasma dilutions starting at 1:100. Cryopreserved human PBMCs from an HIV-seronegative donor with the 158F/V genotype for FcγRIIIa were used as the source of effector cells (71). Data were reported as the proportion of cells positive for proteolytically active granzyme B out of the total viable target cell population after subtracting the background activity observed in wells containing effector and

target cells in the absence of plasma. ADCC endpoint titers were determined by interpolating the dilutions of plasma that intercept the positive cutoff.

Statistical analysis. Pairwise comparisons of assay measurements were performed among the four vaccination groups using Wilcoxon rank-sum tests with exact *P* values. Comparisons were performed between groups with the same vaccine interval (Env protein, prime/boost, and coadministration groups) or between groups with the same vaccine regimen but different vaccine intervals (coadministration and extended interval). Spearman's rank correlation coefficients were calculated and tested with exact *P* values where indicated (Fig. 4 and 7). All statistical analyses were two-tailed, and the *P* values reported were not adjusted for multiple comparisons. The Benjamini-Hochberg step-up procedure was used to determine if any null hypotheses would be rejected for a studywise false discovery rate of 0.05 (72). Data were stored and managed using REDCap, hosted at the Duke University Office of Clinical Research, analysis was performed using SAS 9.3 (SAS Institute, Cary NC), and graphs were created using GraphPad Prism software (version 6; GraphPad, Inc., La Jolla, CA).

SUPPLEMENTAL MATERIAL

Supplemental material for this article may be found at https://doi.org/10.1128/CVI.00231-17.

SUPPLEMENTAL FILE 1, PDF file, 0.1 MB.
SUPPLEMENTAL FILE 2, PDF file, 0.1 MB.
SUPPLEMENTAL FILE 3, PDF file, 0.1 MB.

ACKNOWLEDGMENTS

We gratefully acknowledge the receipt of the CXCR5 antibody from the NIH Nonhuman Primate Reagent Resource, supported by grants number AI126683 and OD010976. The peptide sets for SIVmac239 Gag and the HIV Env consensus C were obtained through the NIH AIDS Reagent Program Division of AIDS, NIAID, NIH. We thank Jennifer Watanabe, Colony Services, and the Pathology, Veterinary, and Clinical Laboratory staff of the California National Primate Research Center for expert technical assistance. This project was supported by the Office of Research Infrastructure Programs/OD (grant number P51OD011107) to CNPRC. We thank Carolyn Weinbaum for her assistance with study coordination; and thank Lawrence C. Armand, Neelima Choudhary, Thaddeus C. Gurley, Caroline L. Jones, Ryan Tuck, and Bob Wilson for expert technical assistance. The UNC Flow Cytometry Core Facility is supported in part by Cancer Center Core support grant number P30 CA016086 to the UNC Lineberger Comprehensive Cancer Center.

Research reported in this publication was supported by the Center for AIDS Research award number 5P30AI050410 and the Louisiana Vaccine Center funded by the Louisiana Board of Regents. The work was supported by grant number P01 AI117915 from the NIAID. The content is solely the responsibility of the authors and does not necessarily represent the official views of the National Institutes of Health.

We thank B. Moss (NIH) for the provision of MVA virus and the recombinant MVA virus expressing SIVmac239 gag-pol.

S.P. and K.D.P. designed the study, K.K.A.V.R. and A.A. were responsible for all animal procedures, D.P. produced the vaccines, B.P. oversaw the study procedures, sample processing and analysis, G.G.F., J.E., E.K., M.D., and X.S. performed the antibody analysis under the leadership of S.P. and M.A.M., P.A.K. analyzed mucosal antibody responses, J.P. and G.F. performed ADCC assays, avidity was assessed by P.A.K. and S.M.A., A.D.C. conducted T follicular helper cell assays, the statistical analysis was performed by C.B. and M.H., and the manuscript was written by B.P., P.A.K., K.K.A.V.R., M.A.M., G.F., S.P., and K.D.P.

REFERENCES

1. UNAIDS. 2016. Prevention gap report. Joint United Nations Programme on HIV/AIDS, Geneva, Switzerland. http://www.unaids.org/sites/default/files/media_asset/2016-prevention-gap-report_en.pdf.
2. UNAIDS. 2016. AIDS by numbers. Joint United Nations Programme on HIV/AIDS, Geneva, Switzerland. http://www.unaids.org/sites/default/files/media_asset/AIDS-by-the-numbers-2016_en.pdf
3. Drake AL, Wagner A, Richardson B, John-Stewart G. 2014. Incident HIV during pregnancy and postpartum and risk of mother-to-child HIV transmission: a systematic review and meta-analysis. PLoS Med 11:e1001608. https://doi.org/10.1371/journal.pmed.1001608.
4. Haas AD, Msukwa MT, Egger M, Tenthani L, Tweya H, Jahn A, Gadabu OJ, Tal K, Salazar-Vizcaya L, Estill J, Spoerri A, Phiri N, Chimbwandira F, van Oosterhout JJ, Keiser O. 2016. Adherence to antiretroviral therapy during and after pregnancy: cohort study on women receiving care in Malawi's

Option B+ Program. Clin Infect Dis 63:1227–1235. https://doi.org/10.1093/cid/ciw500.
5. Myer L, Phillips TK, McIntyre JA, Hsiao NY, Petro G, Zerbe A, Ramjith J, Bekker LG, Abrams EJ. 2017. HIV viraemia and mother-to-child transmission risk after antiretroviral therapy initiation in pregnancy in Cape Town, South Africa. HIV Med 18:80–88. https://doi.org/10.1111/hiv.12397.
6. Tenthani L, Haas AD, Tweya H, Jahn A, van Oosterhout JJ, Chimbwandira F, Chirwa Z, Ng'ambi W, Bakali A, Phiri S, Myer L, Valeri F, Zwahlen M, Wandeler G, Keiser O. 2014. Retention in care under universal antiretroviral therapy for HIV-infected pregnant and breastfeeding women ('Option B+') in Malawi. AIDS 28:589–598. https://doi.org/10.1097/QAD.0000000000000143.
7. WHO. 2014. Global Update on the Health Sector Response to HIV, 2014. World Health Organization, Geneva, Switzerland. http://www.who.int/hiv/pub/progressreports/update2014/en/.
8. Nduati R, John G, Mbori-Ngacha D, Richardson B, Overbaugh J, Mwatha A, Ndinya-Achola J, Bwayo J, Onyango FE, Hughes J, Kreiss J. 2000. Effect of breastfeeding and formula feeding on transmission of HIV-1: a randomized clinical trial. JAMA 283:1167–1174. https://doi.org/10.1001/jama.283.9.1167.
9. Simonich CA, Williams KL, Verkerke HP, Williams JA, Nduati R, Lee KK, Overbaugh J. 2016. HIV-1 neutralizing antibodies with limited hypermutation from an infant. Cell 166:77–87. https://doi.org/10.1016/j.cell.2016.05.055.
10. Goo L, Chohan V, Nduati R, Overbaugh J. 2014. Early development of broadly neutralizing antibodies in HIV-1-infected infants. Nat Med 20:655–658. https://doi.org/10.1038/nm.3565.
11. Pollara J, Bonsignori M, Moody MA, Liu P, Alam SM, Hwang KK, Gurley TC, Kozink DM, Armand LC, Marshall DJ, Whitesides JF, Kaewkungwal J, Nitayaphan S, Pitisuttithum P, Rerks-Ngarm S, Robb ML, O'Connell RJ, Kim JH, Michael NL, Montefiori DC, Tomaras GD, Liao HX, Haynes BF, Ferrari G. 2014. HIV-1 vaccine-induced C1 and V2 Env-specific antibodies synergize for increased antiviral activities. J Virol 88:7715–7726. https://doi.org/10.1128/JVI.00156-14.
12. Tomaras GD, Ferrari G, Shen X, Alam SM, Liao HX, Pollara J, Bonsignori M, Moody MA, Fong Y, Chen X, Poling B, Nicholson CO, Zhang R, Lu X, Parks R, Kaewkungwal J, Nitayaphan S, Pitisuttithum P, Rerks-Ngarm S, Gilbert PB, Kim JH, Michael NL, Montefiori DC, Haynes BF. 2013. Vaccine-induced plasma IgA specific for the C1 region of the HIV-1 envelope blocks binding and effector function of IgG. Proc Natl Acad Sci U S A 110:9019–9024. https://doi.org/10.1073/pnas.1301456110.
13. Ferrari G, Pollara J, Kozink D, Harms T, Drinker M, Freel S, Moody MA, Alam SM, Tomaras GD, Ochsenbauer C, Kappes JC, Shaw GM, Hoxie JA, Robinson JE, Haynes BF. 2011. An HIV-1 gp120 envelope human monoclonal antibody that recognizes a C1 conformational epitope mediates potent antibody-dependent cellular cytotoxicity (ADCC) activity and defines a common ADCC epitope in human HIV-1 serum. J Virol 85:7029–7036. https://doi.org/10.1128/JVI.00171-11.
14. Bonsignori M, Pollara J, Moody MA, Alpert MD, Chen X, Hwang KK, Gilbert PB, Huang Y, Gurley TC, Kozink DM, Marshall DJ, Whitesides JF, Tsao CY, Kaewkungwal J, Nitayaphan S, Pitisuttithum P, Rerks-Ngarm S, Kim JH, Michael NL, Tomaras GD, Montefiori DC, Lewis GK, DeVico A, Evans DT, Ferrari G, Liao HX, Haynes BF. 2012. Antibody-dependent cellular cytotoxicity-mediating antibodies from an HIV-1 vaccine efficacy trial target multiple epitopes and preferentially use the VH1 gene family. J Virol 86:11521–11532. https://doi.org/10.1128/JVI.01023-12.
15. Haynes BF, Gilbert PB, McElrath MJ, Zolla-Pazner S, Tomaras GD, Alam SM, Evans DT, Montefiori DC, Karnasuta C, Sutthent R, Liao HX, DeVico AL, Lewis GK, Williams C, Pinter A, Fong Y, Janes H, DeCamp A, Huang Y, Rao M, Billings E, Karasavvas N, Robb ML, Ngauy V, de Souza MS, Paris R, Ferrari G, Bailer RT, Soderberg KA, Andrews C, Berman PW, Frahm N, De Rosa SC, Alpert MD, Yates NL, Shen X, Koup RA, Pitisuttithum P, Kaewkungwal J, Nitayaphan S, Rerks-Ngarm S, Michael NL, Kim JH. 2012. Immune-correlates analysis of an HIV-1 vaccine efficacy trial. N Engl J Med 366:1275–1286. https://doi.org/10.1056/NEJMoa1113425.
16. Karasavvas N, Billings E, Rao M, Williams C, Zolla-Pazner S, Bailer RT, Koup RA, Madnote S, Arworn D, Shen X, Tomaras GD, Currier JR, Jiang M, Magaret C, Andrews C, Gottardo R, Gilbert P, Cardozo TJ, Rerks-Ngarm S, Nitayaphan S, Pitisuttithum P, Kaewkungwal J, Paris R, Greene K, Gao H, Gurunathan S, Tartaglia J, Sinangil F, Korber BT, Montefiori DC, Mascola JR, Robb ML, Haynes BF, Ngauy V, Michael NL, Kim JH, de Souza MS, the MOPH TAVEG Collaboration. 2012. The Thai phase III HIV type 1 vaccine trial (RV144) regimen induces antibodies that target conserved regions within the V2 loop of gp120. AIDS Res Hum Retroviruses 28:1444–1457. https://doi.org/10.1089/aid.2012.0103.
17. Marthas ML, Miller CJ. 2007. Developing a neonatal HIV vaccine: insights from macaque models of pediatric HIV/AIDS. Curr Opin HIV AIDS 2:367–374. https://doi.org/10.1097/COH.0b013e3282cecf21.
18. Abel K. 2009. The rhesus macaque pediatric SIV infection model—a valuable tool in understanding infant HIV-1 pathogenesis and for designing pediatric HIV-1 prevention strategies. Curr HIV Res 7:2–11. https://doi.org/10.2174/157016209787048528.
19. Fouda GG, Cunningham CK, McFarland EJ, Borkowsky W, Muresan P, Pollara J, Song LY, Liebl BE, Whitaker K, Shen X, Vandergrift NA, Overman RG, Yates NL, Moody MA, Fry C, Kim JH, Michael NL, Robb M, Pitisuttithum P, Kaewkungwal J, Nitayaphan S, Rerks-Ngarm S, Liao HX, Haynes BF, Montefiori DC, Ferrari G, Tomaras GD, Permar SR. 2015. Infant HIV type 1 gp120 vaccination elicits robust and durable anti-V1V2 immunoglobulin G responses and only rare envelope-specific immunoglobulin A responses. J Infect Dis 211:508–517. https://doi.org/10.1093/infdis/jiu444.
20. Jensen K, Nabi R, Van Rompay KK, Robichaux S, Lifson JD, Piatak M, Jr, Jacobs WR, Jr, Fennelly G, Canfield D, Mollan KR, Hudgens MG, Larsen MH, Amedee AM, Kozlowski PA, De Paris K. 2016. Vaccine-elicited mucosal and systemic antibody responses are associated with reduced simian immunodeficiency viremia in infant rhesus macaques. J Virol 90:7285–7302. https://doi.org/10.1128/JVI.00481-16.
21. Rerks-Ngarm S, Pitisuttithum P, Nitayaphan S, Kaewkungwal J, Chiu J, Paris R, Premsri N, Namwat C, de Souza M, Adams E, Benenson M, Gurunathan S, Tartaglia J, McNeil JG, Francis DP, Stablein D, Birx DL, Chunsuttiwat S, Khamboonruang C, Thongcharoen P, Robb ML, Michael NL, Kunasol P, Kim JH, MOPH-TAVEG Investigators. 2009. Vaccination with ALVAC and AIDSVAX to prevent HIV-1 infection in Thailand. N Engl J Med 361:2209–2220. https://doi.org/10.1056/NEJMoa0908492.
22. McFarland EJ, Johnson DC, Muresan P, Fenton T, Tomaras GD, McNamara J, Read JS, Douglas SD, Deville J, Gurwith M, Gurunathan S, Lambert JS. 2006. HIV-1 vaccine induced immune responses in newborns of HIV-1 infected mothers. AIDS 20:1481–1489. https://doi.org/10.1097/01.aids.0000237363.33994.45.
23. Van Rompay KK, Abel K, Lawson JR, Singh RP, Schmidt KA, Evans T, Earl P, Harvey D, Franchini G, Tartaglia J, Montefiori D, Hattangadi S, Moss B, Marthas ML. 2005. Attenuated poxvirus-based simian immunodeficiency virus (SIV) vaccines given in infancy partially protect infant and juvenile macaques against repeated oral challenge with virulent SIV. J Acquir Immune Defic Syndr 38:124–134. https://doi.org/10.1097/00126334-200502010-00002.
24. Odutola AA, Owolabi OA, Owiafe PK, McShane H, Ota MO. 2012. A new TB vaccine, MVA85A, induces durable antigen-specific responses 14 months after vaccination in African infants. Vaccine 30:5591–5594. https://doi.org/10.1016/j.vaccine.2012.06.054.
25. Tameris M, Geldenhuys H, Luabeya AK, Smit E, Hughes JE, Vermaak S, Hanekom WA, Hatherill M, Mahomed H, McShane H, Scriba TJ. 2014. The candidate TB vaccine, MVA85A, induces highly durable Th1 responses. PLoS One 9:e87340. https://doi.org/10.1371/journal.pone.0087340.
26. Zolla-Pazner S, deCamp AC, Cardozo T, Karasavvas N, Gottardo R, Williams C, Morris DE, Tomaras G, Rao M, Billings E, Berman P, Shen X, Andrews C, O'Connell RJ, Ngauy V, Nitayaphan S, de Souza M, Korber B, Koup R, Bailer RT, Mascola JR, Pinter A, Montefiori D, Haynes BF, Robb ML, Rerks-Ngarm S, Michael NL, Gilbert PB, Kim JH. 2013. Analysis of V2 antibody responses induced in vaccinees in the ALVAC/AIDSVAX HIV-1 vaccine efficacy trial. PLoS One 8:e53629. https://doi.org/10.1371/journal.pone.0053629.
27. Montefiori DC, Karnasuta C, Huang Y, Ahmed H, Gilbert P, de Souza MS, McLinden R, Tovanabutra S, Laurence-Chenine A, Sanders-Buell E, Moody MA, Bonsignori M, Ochsenbauer C, Kappes J, Tang H, Greene K, Gao H, LaBranche CC, Andrews C, Polonis VR, Rerks-Ngarm S, Pitisuttithum P, Nitayaphan S, Kaewkungwal J, Self SG, Berman PW, Francis D, Sinangil F, Lee C, Tartaglia J, Robb ML, Haynes BF, Michael NL, Kim JH. 2012. Magnitude and breadth of the neutralizing antibody response in the RV144 and Vax003 HIV-1 vaccine efficacy trials. J Infect Dis 206:431–441. https://doi.org/10.1093/infdis/jis367.
28. Permar SR, Fong Y, Vandergrift N, Fouda GG, Gilbert P, Parks R, Jaeger FH, Pollara J, Martelli A, Liebl BE, Lloyd K, Yates NL, Overman RG, Shen X, Whitaker K, Chen H, Pritchett J, Solomon E, Friberg E, Marshall DJ, Whitesides JF, Gurley TC, Von Holle T, Martinez DR, Cai F, Kumar A, Xia SM, Lu X, Louzao R, Wilkes S, Datta S, Sarzotti-Kelsoe M, Liao HX, Ferrari G, Alam SM, Montefiori DC, Denny TN, Moody MA, Tomaras GD, Gao F,

Haynes BF. 2015. Maternal HIV-1 envelope-specific antibody responses and reduced risk of perinatal transmission. J Clin Invest 125:2702–2706. https://doi.org/10.1172/JCI81593.
29. Marthas ML, Van Rompay KK, Abbott Z, Earl P, Buonocore-Buzzelli L, Moss B, Rose NF, Rose JK, Kozlowski PA, Abel K. 2011. Partial efficacy of a VSV-SIV/MVA-SIV vaccine regimen against oral SIV challenge in infant macaques. Vaccine 29:3124–3137. https://doi.org/10.1016/j.vaccine.2011.02.051.
30. Lai L, Vodros D, Kozlowski PA, Montefiori DC, Wilson RL, Akerstrom VL, Chennareddi L, Yu T, Kannanganat S, Ofielu L, Villinger F, Wyatt LS, Moss B, Amara RR, Robinson HL. 2007. GM-CSF DNA: an adjuvant for higher avidity IgG, rectal IgA, and increased protection against the acute phase of a SHIV-89.6P challenge by a DNA/MVA immunodeficiency virus vaccine. Virology 369:153–167. https://doi.org/10.1016/j.virol.2007.07.017.
31. Pegu P, Vaccari M, Gordon S, Keele BF, Doster M, Guan Y, Ferrari G, Pal R, Ferrari MG, Whitney S, Hudacik L, Billings E, Rao M, Montefiori D, Tomaras G, Alam SM, Fenizia C, Lifson JD, Stablein D, Tartaglia J, Michael N, Kim J, Venzon D, Franchini G. 2013. Antibodies with high avidity to the gp120 envelope protein in protection from simian immunodeficiency virus SIV(mac251) acquisition in an immunization regimen that mimics the RV-144 Thai trial. J Virol 87:1708–1719. https://doi.org/10.1128/JVI.02544-12.
32. Cole KS, Murphey-Corb M, Narayan O, Joag SV, Shaw GM, Montelaro RC. 1998. Common themes of antibody maturation to simian immunodeficiency virus, simian-human immunodeficiency virus, and human immunodeficiency virus type 1 infections. J Virol 72:7852–7859.
33. Van Rompay KK, Abel K, Earl P, Kozlowski PA, Easlick J, Moore J, Buonocore-Buzzelli L, Schmidt KA, Wilson RL, Simon I, Moss B, Rose N, Rose J, Marthas ML. 2010. Immunogenicity of viral vector, prime-boost SIV vaccine regimens in infant rhesus macaques: attenuated vesicular stomatitis virus (VSV) and modified vaccinia Ankara (MVA) recombinant SIV vaccines compared to live-attenuated SIV. Vaccine 28:1481–1492. https://doi.org/10.1016/j.vaccine.2009.11.061.
34. Jensen K, Pena MG, Wilson RL, Ranganathan UD, Jacobs WR, Jr, Fennelly G, Larsen M, Van Rompay KK, Kozlowski PA, Abel K. 2013. A neonatal oral Mycobacterium tuberculosis-SIV prime/intramuscular MVA-SIV boost combination vaccine induces both SIV and Mtb-specific immune responses in infant macaques. Trials Vaccinol 2:53–63. https://doi.org/10.1016/j.trivac.2013.09.005.
35. Xiao P, Zhao J, Patterson LJ, Brocca-Cofano E, Venzon D, Kozlowski PA, Hidajat R, Demberg T, Robert-Guroff M. 2010. Multiple vaccine-elicited nonneutralizing antienvelope antibody activities contribute to protective efficacy by reducing both acute and chronic viremia following simian/human immunodeficiency virus SHIV89.6P challenge in rhesus macaques. J Virol 84:7161–7173. https://doi.org/10.1128/JVI.00410-10.
36. Adnan S, Reeves RK, Gillis J, Wong FE, Yu Y, Camp JV, Li Q, Connole M, Li Y, Piatak M, Jr, Lifson JD, Li W, Keele BF, Kozlowski PA, Desrosiers RC, Haase AT, Johnson RP. 2016. Persistent low-level replication of SIVDeltanef drives maturation of antibody and CD8 T cell responses to induce protective immunity against vaginal SIV infection. PLoS Pathog 12:e1006104. https://doi.org/10.1371/journal.ppat.1006104.
37. Xiao P, Patterson LJ, Kuate S, Brocca-Cofano E, Thomas MA, Venzon D, Zhao J, DiPasquale J, Fenizia C, Lee EM, Kalisz I, Kalyanaraman VS, Pal R, Montefiori D, Keele BF, Robert-Guroff M. 2012. Replicating adenovirus-simian immunodeficiency virus (SIV) recombinant priming and envelope protein boosting elicits localized, mucosal IgA immunity in rhesus macaques correlated with delayed acquisition following a repeated low-dose rectal SIV(mac251) challenge. J Virol 86:4644–4657. https://doi.org/10.1128/JVI.06812-11.
38. Binley JM, Arshad H, Fouts TR, Moore JP. 1997. An investigation of the high-avidity antibody response to glycoprotein 120 of human immunodeficiency virus type 1. AIDS Res Hum Retroviruses 13:1007–1015. https://doi.org/10.1089/aid.1997.13.1007.
39. Kim JH, Excler JL, Michael NL. 2015. Lessons from the RV144 Thai phase III HIV-1 vaccine trial and the search for correlates of protection. Annu Rev Med 66:423–437. https://doi.org/10.1146/annurev-med-052912-123749.
40. Gilbert PB, Peterson ML, Follmann D, Hudgens MG, Francis DP, Gurwith M, Heyward WL, Jobes DV, Popovic V, Self SG, Sinangil F, Burke D, Berman PW. 2005. Correlation between immunologic responses to a recombinant glycoprotein 120 vaccine and incidence of HIV-1 infection in a phase 3 HIV-1 preventive vaccine trial. J Infect Dis 191:666–677. https://doi.org/10.1086/428405.
41. Karnasuta C, Akapirat S, Madnote S, Savadsuk H, Puangkaew J, Rittiroongrad S, Rerks-Ngarm S, Nitayaphan S, Pitisuttithum P, Kaewkungwal J, Tartaglia J, Sinangil F, Francis DP, Robb ML, de Souza MS, Michael NL, Excler JL, Kim JH, O'Connell RJ, Karasavvas N. 2017. Comparison of antibody responses induced by RV144, VAX003, and VAX004 vaccination regimens. AIDS Res Hum Retroviruses 33:410–423. https://doi.org/10.1089/aid.2016.0204.
42. Bomsel M, Tudor D, Drillet AS, Alfsen A, Ganor Y, Roger MG, Mouz N, Amacker M, Chalifour A, Diomede L, Devillier G, Cong Z, Wei Q, Gao H, Qin C, Yang GB, Zurbriggen R, Lopalco L, Fleury S. 2011. Immunization with HIV-1 gp41 subunit virosomes induces mucosal antibodies protecting nonhuman primates against vaginal SHIV challenges. Immunity 34:269–280. https://doi.org/10.1016/j.immuni.2011.01.015.
43. Rosario M, Fulkerson J, Soneji S, Parker J, Im EJ, Borthwick N, Bridgeman A, Bourne C, Joseph J, Sadoff JC, Hanke T. 2010. Safety and immunogenicity of novel recombinant BCG and modified vaccinia virus Ankara vaccines in neonate rhesus macaques. J Virol 84:7815–7821. https://doi.org/10.1128/JVI.00726-10.
44. Omenda MM, Milligan C, Odem-Davis K, Nduati R, Richardson BA, Lynch J, John-Stewart G, Overbaugh J. 2013. Evidence for efficient vertical transfer of maternal HIV-1 envelope-specific neutralizing antibodies but no association of such antibodies with reduced infant infection. J Acquir Immune Defic Syndr 64:163–166. https://doi.org/10.1097/QAI.0b013e31829f6e41.
45. Jackson AG, Else LJ, Mesquita PM, Egan D, Back DJ, Karolia Z, Ringner-Nackter L, Higgs CJ, Herold BC, Gazzard BG, Boffito M. 2014. A compartmental pharmacokinetic evaluation of long-acting rilpivirine in HIV-negative volunteers for pre-exposure prophylaxis. Clin Pharmacol Ther 96:314–323. https://doi.org/10.1038/clpt.2014.118.
46. Fouda GG, Amos JD, Wilks AB, Pollara J, Ray CA, Chand A, Kunz EL, Liebl BE, Whitaker K, Carville A, Smith S, Colvin L, Pickup DJ, Staats HF, Overman G, Eutsey-Lloyd K, Parks R, Chen H, Labranche C, Barnett S, Tomaras GD, Ferrari G, Montefiori DC, Liao HX, Letvin NL, Haynes BF, Permar SR. 2013. Mucosal immunization of lactating female rhesus monkeys with a transmitted/founder HIV-1 envelope induces strong Env-specific IgA antibody responses in breast milk. J Virol 87:6986–6999. https://doi.org/10.1128/JVI.00528-13.
47. Staib C, Drexler I, Sutter G. 2004. Construction and isolation of recombinant MVA. Methods Mol Biol 269:77–100. https://doi.org/10.1385/1-59259-789-0:077.
48. Earl PL, Wyatt LS, Montefiori DC, Bilska M, Woodward R, Markham PD, Malley JD, Vogel TU, Allen TM, Watkins DI, Miller N, Moss B. 2002. Comparison of vaccine strategies using recombinant env-gag-pol MVA with or without an oligomeric Env protein boost in the SHIV rhesus macaque model. Virology 294:270–281. https://doi.org/10.1006/viro.2001.1345.
49. National Research Council. 2011. Guide for the care and use of laboratory animals, 8th ed. National Academies Press, Washington, DC.
50. Council for International Organization of Medical Sciences and The International Council for Laboratory Animal Science. 2012. International guiding principles for biomedical research involving animals. http://issuu.com/aaalac/docs/igp2012.
51. Moody MA, Santra S, Vandergrift NA, Sutherland LL, Gurley TC, Drinker MS, Allen AA, Xia SM, Meyerhoff RR, Parks R, Lloyd KE, Easterhoff D, Alam SM, Liao HX, Ward BM, Ferrari G, Montefiori DC, Tomaras GD, Seder RA, Letvin NL, Haynes BF. 2014. Toll-like receptor 7/8 (TLR7/8) and TLR9 agonists cooperate to enhance HIV-1 envelope antibody responses in rhesus macaques. J Virol 88:3329–3339. https://doi.org/10.1128/JVI.03309-13.
52. Blackwood RS, Tarara RP, Christe KL, Spinner A, Lerche NW. 2008. Effects of the macrolide drug tylosin on chronic diarrhea in rhesus macaques (Macaca mulatta). Comp Med 58:81–87. http://europepmc.org/abstract/MED/19793461.
53. Nikolaenko IV, Galkin A, Raevskaia GE, Kas'ianenko TV, Nereshchenko MI, Donskaia ES, Spivak N. 2005. Preparation of monoclonal antibodies to the Fc-fragment of human IgG and the use of their based immunoenzyme conjugates. Klin Lab Diagn 2005:8–11. (In Russian.)
54. Davis KL, Bibollet-Ruche F, Li H, Decker JM, Kutsch O, Morris L, Salomon A, Pinter A, Hoxie JA, Hahn BH, Kwong PD, Shaw GM. 2009. Human immunodeficiency virus type 2 (HIV-2)/HIV-1 envelope chimeras detect high titers of broadly reactive HIV-1 V3-specific antibodies in human plasma. J Virol 83:1240–1259. https://doi.org/10.1128/JVI.01743-08.
55. Gottardo R, Bailer RT, Korber BT, Gnanakaran S, Phillips J, Shen X, Tomaras GD, Turk E, Imholte G, Eckler L, Wenschuh H, Zerweck J, Greene K, Gao H, Berman PW, Francis D, Sinangil F, Lee C, Nitayaphan S,

Rerks-Ngarm S, Kaewkungwal J, Pitisuttithum P, Tartaglia J, Robb ML, Michael NL, Kim JH, Zolla-Pazner S, Haynes BF, Mascola JR, Self S, Gilbert P, Montefiori DC. 2013. Plasma IgG to linear epitopes in the V2 and V3 regions of HIV-1 gp120 correlate with a reduced risk of infection in the RV144 vaccine efficacy trial. PLoS One 8:e75665. https://doi.org/10.1371/journal.pone.0075665.

56. Liu P, Overman RG, Yates NL, Alam SM, Vandergrift N, Chen Y, Graw F, Freel SA, Kappes JC, Ochsenbauer C, Montefiori DC, Gao F, Perelson AS, Cohen MS, Haynes BF, Tomaras GD. 2011. Dynamic antibody specificities and virion concentrations in circulating immune complexes in acute to chronic HIV-1 infection. J Virol 85:11196–11207. https://doi.org/10.1128/JVI.05601-11.
57. Nelson CS, Pollara J, Kunz EL, Jeffries TL, Jr, Duffy R, Beck C, Stamper L, Wang M, Shen X, Pickup DJ, Staats HF, Hudgens MG, Kepler TB, Montefiori DC, Moody MA, Tomaras GD, Liao HX, Haynes BF, Ferrari G, Fouda GG, Permar SR. 2016. Combined HIV-1 envelope systemic and mucosal immunization of lactating rhesus monkeys induces a robust immunoglobulin A isotype B cell response in breast milk. J Virol 90:4951–4965. https://doi.org/10.1128/JVI.00335-16.
58. Pollara J, McGuire E, Fouda GG, Rountree W, Eudailey J, Overman RG, Seaton KE, Deal A, Edwards RW, Tegha G, Kamwendo D, Kumwenda J, Nelson JA, Liao HX, Brinkley C, Denny TN, Ochsenbauer C, Ellington S, King CC, Jamieson DJ, van der Horst C, Kourtis AP, Tomaras GD, Ferrari G, Permar SR. 2015. Association of HIV-1 envelope-specific breast milk IgA responses with reduced risk of postnatal mother-to-child transmission of HIV-1. J Virol 89:9952–9961. https://doi.org/10.1128/JVI.01560-15.
59. Tomaras GD, Yates NL, Liu P, Qin L, Fouda GG, Chavez LL, Decamp AC, Parks RJ, Ashley VC, Lucas JT, Cohen M, Eron J, Hicks CB, Liao HX, Self SG, Landucci G, Forthal DN, Weinhold KJ, Keele BF, Hahn BH, Greenberg ML, Morris L, Karim SS, Blattner WA, Montefiori DC, Shaw GM, Perelson AS, Haynes BF. 2008. Initial B-cell responses to transmitted human immunodeficiency virus type 1: virion-binding immunoglobulin M (IgM) and IgG antibodies followed by plasma anti-gp41 antibodies with ineffective control of initial viremia. J Virol 82:12449–12463. https://doi.org/10.1128/JVI.01708-08.
60. Fouda GG, Eudailey J, Kunz EL, Amos JD, Liebl BE, Himes J, Boakye-Agyeman F, Beck K, Michaels AJ, Cohen-Wolkowiez M, Haynes BF, Reimann KA, Permar SR. 2017. Systemic administration of an HIV-1 broadly neutralizing dimeric IgA yields mucosal secretory IgA and virus neutralization. Mucosal Immunol 10:228–237. https://doi.org/10.1038/mi.2016.32.
61. Tomaras GD, Binley JM, Gray ES, Crooks ET, Osawa K, Moore PL, Tumba N, Tong T, Shen X, Yates NL, Decker J, Wibmer CK, Gao F, Alam SM, Easterbrook P, Abdool Karim S, Kamanga G, Crump JA, Cohen M, Shaw GM, Mascola JR, Haynes BF, Montefiori DC, Morris L. 2011. Polyclonal B cell responses to conserved neutralization epitopes in a subset of HIV-1-infected individuals. J Virol 85:11502–11519. https://doi.org/10.1128/JVI.05363-11.
62. Shen X, Duffy R, Howington R, Cope A, Sadagopal S, Park H, Pal R, Kwa S, Ding S, Yang OO, Fouda GG, Le Grand R, Bolton D, Esteban M, Phogat S, Roederer M, Amara RR, Picker LJ, Seder RA, McElrath MJ, Barnett S, Permar SR, Shattock R, DeVico AL, Felber BK, Pavlakis GN, Pantaleo G, Korber BT, Montefiori DC, Tomaras GD. 2015. Vaccine-induced linear epitope-specific antibodies to simian immunodeficiency virus SIVmac239 envelope are distinct from those induced to the human immunodeficiency virus type 1 envelope in nonhuman primates. J Virol 89:8643–8650. https://doi.org/10.1128/JVI.03635-14.
63. Iyer SS, Gangadhara S, Victor B, Shen X, Chen X, Nabi R, Kasturi SP, Sabula MJ, Labranche CC, Reddy PB, Tomaras GD, Montefiori DC, Moss B, Spearman P, Pulendran B, Kozlowski PA, Amara RR. 2016. Virus-like particles displaying trimeric simian immunodeficiency virus (SIV) envelope gp160 enhance the breadth of DNA/modified vaccinia virus Ankara SIV vaccine-induced antibody responses in rhesus macaques. J Virol 90:8842–8854. https://doi.org/10.1128/JVI.01163-16.
64. Bilello JP, Manrique JM, Shin YC, Lauer W, Li W, Lifson JD, Mansfield KG, Johnson RP, Desrosiers RC. 2011. Vaccine protection against simian immunodeficiency virus in monkeys using recombinant gamma-2 herpesvirus. J Virol 85:12708–12720. https://doi.org/10.1128/JVI.00865-11.
65. Montefiori DC. 2009. Measuring HIV neutralization in a luciferase reporter gene assay. Methods Mol Biol 485:395–405. https://doi.org/10.1007/978-1-59745-170-3_26.
66. Silveira EL, Kasturi SP, Kovalenkov Y, Rasheed AU, Yeiser P, Jinnah ZS, Legere TH, Pulendran B, Villinger F, Wrammert J. 2015. Vaccine-induced plasmablast responses in rhesus macaques: phenotypic characterization and a source for generating antigen-specific monoclonal antibodies. J Immunol Methods 416:69–83. https://doi.org/10.1016/j.jim.2014.11.003.
67. Fan Q, Nelson CS, Bialas KM, Chiuppesi F, Amos J, Gurley TC, Marshall DJ, Eudailey J, Heimsath H, Himes J, Deshpande A, Walter MR, Wussow F, Diamond DJ, Barry PA, Moody MA, Kaur A, Permar SR. 2017. Plasmablast response to primary rhesus cytomegalovirus (CMV) infection in a monkey model of congenital CMV transmission. Clin Vaccine Immunol 24:e00510-16. https://doi.org/10.1128/CVI.00510-16.
68. Moody MA, Yates NL, Amos JD, Drinker MS, Eudailey JA, Gurley TC, Marshall DJ, Whitesides JF, Chen X, Foulger A, Yu JS, Zhang R, Meyerhoff RR, Parks R, Scull JC, Wang L, Vandergrift NA, Pickeral J, Pollara J, Kelsoe G, Alam SM, Ferrari G, Montefiori DC, Voss G, Liao HX, Tomaras GD, Haynes BF. 2012. HIV-1 gp120 vaccine induces affinity maturation in both new and persistent antibody clonal lineages. J Virol 86:7496–7507. https://doi.org/10.1128/JVI.00426-12.
69. Jensen K, Dela Pena-Ponce MG, Piatak M, Jr, Shoemaker R, Oswald K, Jacobs WR, Jr, Fennelly G, Lucero C, Mollan KR, Hudgens MG, Amedee A, Kozlowski PA, Estes JD, Lifson JD, Van Rompay KK, Larsen M, De Paris K. 2017. Balancing trained immunity with persistent immune activation and the risk of SIV infection in infant macaques vaccinated with attenuated Mycobacterium tuberculosis or BCG vaccines. Clin Vaccine Immunol 24:e00360-16. https://doi.org/10.1128/CVI.00360-16.
70. Pollara J, Hart L, Brewer F, Pickeral J, Packard BZ, Hoxie JA, Komoriya A, Ochsenbauer C, Kappes JC, Roederer M, Huang Y, Weinhold KJ, Tomaras GD, Haynes BF, Montefiori DC, Ferrari G. 2011. High-throughput quantitative analysis of HIV-1 and SIV-specific ADCC-mediating antibody responses. Cytometry A 79:603–612. https://doi.org/10.1002/cyto.a.21084.
71. Koene HR, Kleijer M, Algra J, Roos D, von dem Borne AE, de Haas M. 1997. Fc gammaRIIIa-158V/F polymorphism influences the binding of IgG by natural killer cell Fc gammaRIIIa, independently of the Fc gammaRIIIa-48L/R/H phenotype. Blood 90:1109–1114.
72. Benjamini Y, Hochberg Y. 1995. Controlling the false discovery rate: a practical and powerful approach to multiple testing. J R Stat Soc Ser B Methodol 57:289–300. http://www.jstor.org/stable/2346101.